National Physical Laboratory

NPL REPORT ENG 32

An overview of industrial X-ray computed tomography

Sun W, Brown S B and Leach R K

JANUARY 2012

National Measurement System

An overview of industrial X-ray computed tomography

Sun W, Brown S B and Leach R K
Engineering Measurement Division

ABSTRACT

Driven by the need for quality control of complex three-dimensional engineering components, and enabled by progress in medical imaging and consumer graphics processing, X-ray computed tomography (XCT) has been increasingly used for industrial inspection in recent years. A review of the recent development of industrial XCT systems in the context of traceable dimensional metrology is presented. The market trends of industrial XCT systems are briefly reviewed. Progress towards standards and methods for XCT calibration and verification are studied in detail. The report also covers the recent development of both hardware and software and discusses the challenges regarding systematic errors. Commercial systems are summarised to establish the capability available to the industrial user. Finally, what will be required to develop XCT technology in the field of dimensional metrology is considered.

ISSN 1754-2987

National Physical Laboratory
Hampton Road, Teddington, Middlesex, TW11 0LW

Approved on behalf of NPLML by Dr A J Lewis, Assistant Knowledge Leader.

CONTENTS

FIGURES

TABLES

1 INTRODUCTION

X-ray computed tomography, abbreviated as XCT or CT, uses X-rays to take multiple two dimensional (2D) transmission images of an object from different orientations. These images are then processed, using computers, to construct a three dimensional (3D) image of the object, including its interior geometry. The word 'tomography' is derived from two Greek words, '*tomos*' meaning 'slice' — images are taken through the volume of the object — and '*graphein*' meaning 'to write' or record the image.

The idea that the inside structure of an object could be determined from multiple X-ray images and from various angles around that object was developed by Godfrey Hounsfield while working for EMI in the UK [1]. Hounsfield was not aware that, at the same time he was developing his system, Allan Cormack from Tufts University in the USA was working on the theory for such a device. In 1979, Hounsfield and Cormack were awarded the Nobel Prize for Physiology or Medicine, in recognition of the development of XCT. The 'Hounsfield' was subsequently introduced in the medical field as a unit for the measurement of radiodensity, or the absorption of X-rays as they pass through a given material [2]. The Hounsfield is given the symbol HU and is defined such that the radiodensity of distilled water at standard temperature and pressure (STP) is equal to zero Hounsfield units (HU), while the radiodensity of air at STP is equal to -1000 HU. On this scale, compact bone has a value of +1000 HU.

XCT systems have been in existence since the 1970s and were first used in medical imaging to supplement 2D X-ray images (also known as radiographs) and ultrasound. Although XCT and magnetic resonance imaging (MRI) techniques are similar, in that both employ electromagnetic radiation, they differ in that XCT uses ionizing radiation whereas MRI uses non-ionizing radiation, for example radio frequency radiation. XCT relies on absorption of X-rays, whereas MRI uses the magnetic resonance of hydrogen molecules. Consequently, both techniques have different areas of application. XCT is a useful tool for examining compounds of elements with high atomic number whereas MRI is used in examining soft animal tissue.

In the area generally referred to as medical XCT, systems can be used as full body scanners or in the targeted investigation of parts of the body, head, lungs, heart, *etc*. Although there are many advantages from the use of XCT systems, there is also the disadvantage that exposure to radiation may cause cancers. It is reported [3] that, in the United States in 2007, seventy-two million scans were carried out and that 0.4 % of current cancers are due to XCT scans preformed in the past, with this figure rising to as high as 1.5 % to 2 % with the current rate of XCT scans. Knowing, through calibration, the correct dosage to apply will help dramatically reduce the risk of initiating cancers.

Another area of use for XCT is classed as 'industrial XCT scanning' where it is used in the detection of material flaws such as voids, cracks and for dimensional measurements. With advances in software, the capability of XCT as a metrology tool has grown to allow measurements of the internal and external geometry of complex parts. Prior to the use of XCT systems, to measure internal dimensions, companies relied on either disassembly or destructive testing of the object. XCT systems can measure these objects and verify that they conform to the original design specification.

This report is a review of the application of XCT as a measuring tool for industrial applications. This review will highlight trends, from current and emerging markets and areas where XCT systems are used as a metrology tool. The review will highlight the need for traceability of XCT systems, including some current work in this field. An overview of the hardware and software that make up XCT systems is included. Some known errors, random and systematic, will be discussed. An overview of some of the XCT systems that are currently available on the market will be listed. The review will finally draw a conclusion to its findings and highlight areas that it deems need further research work.

1.1 THE X-RAY SPECTRUM AND XCT SYSTEMS

XCT systems rely on the use of X-rays for imaging. X-rays are a form of electromagnetic radiation with a wavelength in the range of approximately 10 nm to 0.01 nm and a photon energy ranging from 0.12 keV to 120 keV(see figure 1). X-rays can penetrate visibly opaque materials and are not significantly deflected by lenses designed for visible light. As with all electromagnetic radiation, X-rays are also negligibly affected by electric or magnetic fields and continue to propagate in straight lines.

X-rays are divided into two categories: ‘soft’ X-rays which have the energy range of 0.12 keV to 12 keV and ‘hard’ X-rays which cover the higher energy range of 12 keV to 120 keV. An increase in the X-ray tube voltage increases the energy of each X-ray photon emitted. An increase in the electrical current increases the number of X-ray photons produced. The energy of the X-ray photon determines its penetration capability, and the quantity determines the exposure to the radiation. Soft X-rays are usually referred to as non-penetrating and are typically removed by the placement of a filter, generally of a material such as aluminium foil.

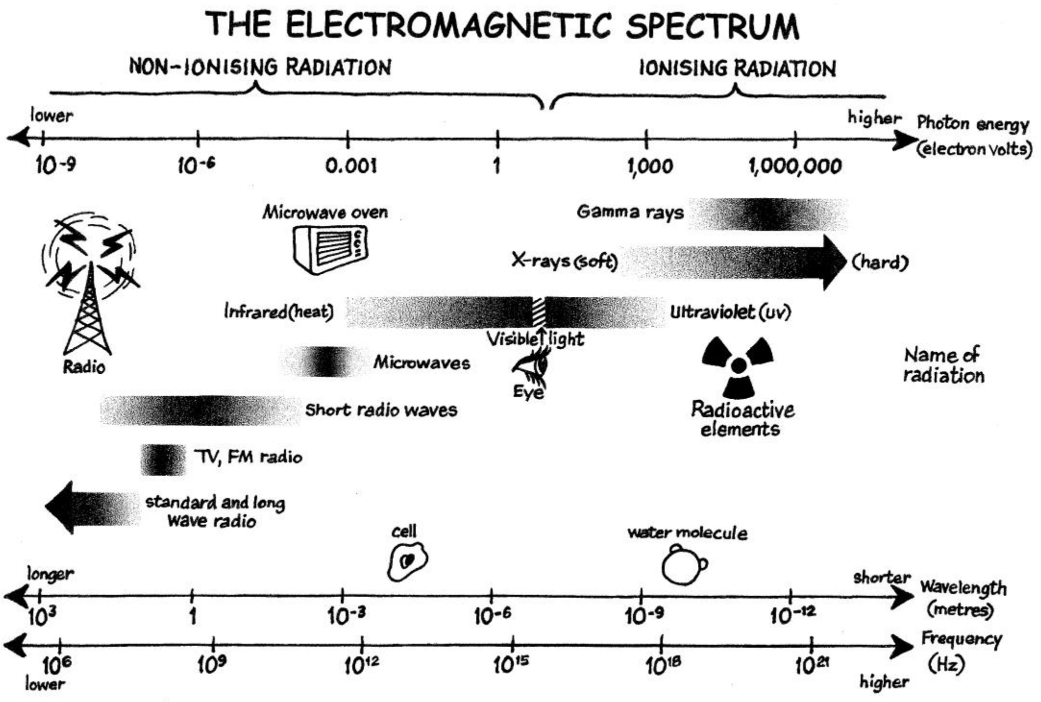

Figure 1. The electromagnetic spectrum [4]

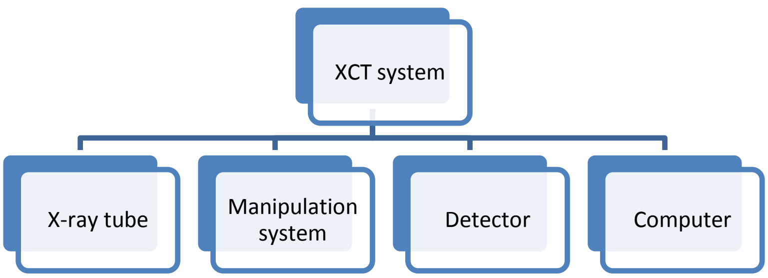

Figure 2. Structure of XCT systems

An XCT system usually consists of an X-ray source, a sample manipulation system, a radiation detector and a computer system to analyse data. Figure 2 shows the structure of XCT systems. In operation, an X-ray tube emits an X-ray beam. The detector collects projection images of the sample from different angles when either the sample or the X-ray source and the detector rotate. The data can then be analysed in a computer and the image of the sample under test reconstructed.

1.2 CLASSIFICATION OF INDUSTRIAL XCT SYSTEMS

According to the shape of the X-ray beam, industrial XCT systems on the market can be divided into fan/line beam scanners and cone beam scanners, and then subdivided into their energy range.

- Fan/line beam scanners

Fan/line beam scanners were the first generation X-ray scanners and employ the use of a beam of X-rays to scan through the volume of the object as it is rotated (see figure 3). All of the resulting 2D slices are then used to construct a 3D representation of the object. Fan beam tomography (2D tomography) tends to use linear X-ray detectors.

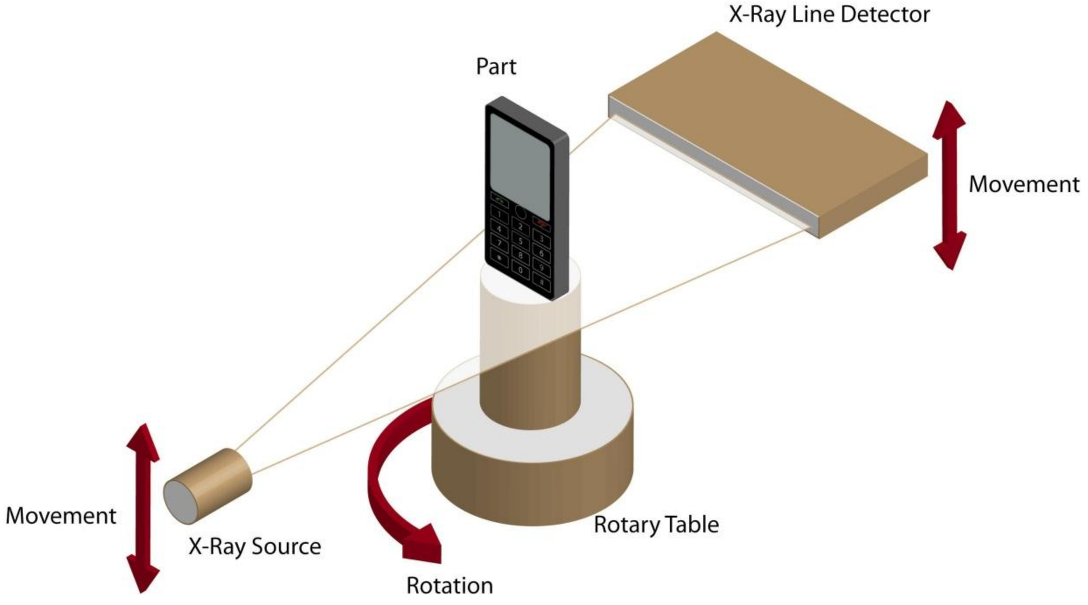

Figure 3. A line beam scanner

- Cone beam scanners

Cone beam scanners use a cone beam of X-rays (see figure 4), to take over a thousand images of the object as it is rotated around a fixed axis. These 2D images are then processed to create a 3D reconstruction of the object (see section 4.1). These scanners tend to use 2D flat panel X-ray detectors. In most cases the projected beam passes through the object and onto a detector. The reconstruction method is usually based on the Feldkamp algorithm (FDK) [5]. Information on image reconstruction is discussed in section 4.1.

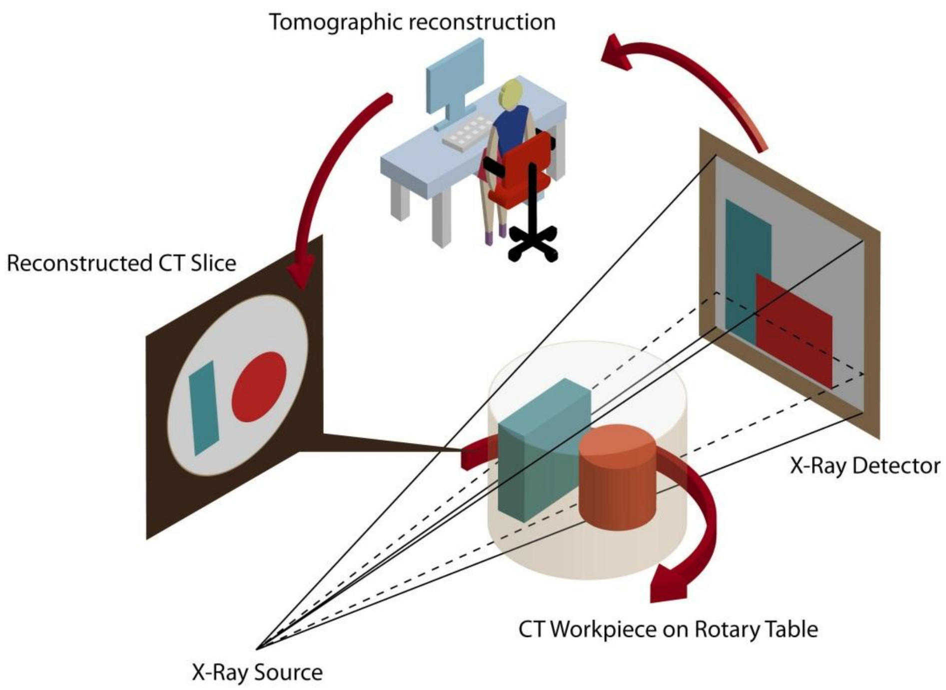

Figure 4. A typical cone beam scanner

- Energy range

There are generally four energy levels for XCT systems, which are commonly grouped by their source energy (here energy is expressed in units of electron-volts) and these are summarised in table 1. For an overview of resolution, please refer to sections 3.3 and 6.4.1.

Table 1. XCT classification

Type	Energy range	Resolution
Nano	n/a	< 1 µm
Low-power	0 to –110 keV	> 1 µm
Mid-power	110 keV to –999 keV	> 1 µm
High-power	> 1 MeV	> 1 µm

1.3 ADVANTAGES OF XCT

XCT systems are beginning to surpass conventional tactile co-ordinate measuring machines (CMMs) or laser scanners in some areas due to advantages that are listed below:

- capability for non-destructive-testing (NDT) for inspection and metrology;
- significant reduction of inspection and analysis costs from first article to production;
- ability to quickly and accurately validate design requirements for both internal and external components;
- precision measurement of complex internal features without destructive testing;
- fixture requirements - parts are scanned in a free-standing state, minimising risk of damage or clamping deformation errors;
- ability to reverse engineer enclosed geometries and components; and
- reduction in development costs in creating the first CAD model.

1.4 ANALYSIS AND INSPECTION

XCT systems generate volumetric images from 2D images of the object under investigation where these image stacks are individually referred to as radiographs (see figure 5). By reconstructing the image stacks (see section 4) the volumetric image is constructed. A voxel is a unit of graphical information that defines a point in a 3D space. In the case of an XCT scan, a voxel also has a value that represents the density of the material at the point represented by the voxel.

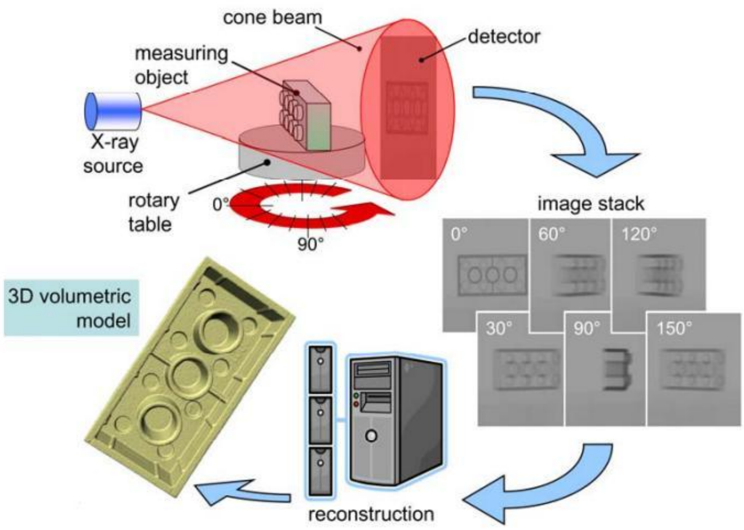

Figure 5. XCT reconstruction, from [6]

Measurements can be performed on individual parts or the assembly of parts, with comparisons easily made with the original design drawings (CAD models). Colour-coded deviation plots (see an example in figure 6) facilitate rapid visual inspection of the object, often saving time and cost. One of the advantages of XCT over alternative inspection techniques is the fact that failed objects (for example a pump) can be scanned in their failed state without the need to disassemble the part - disassembly might cause further failures that could disguise the initial problem.

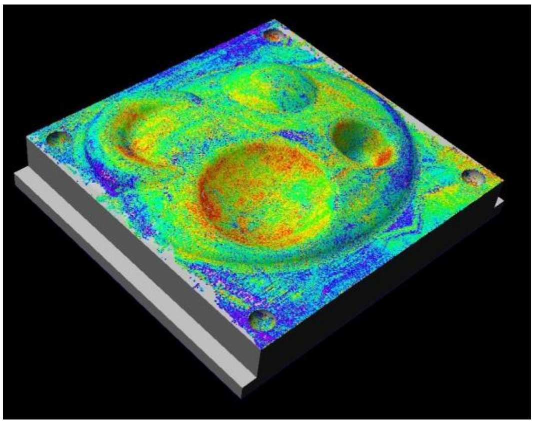

Figure 6. Typical output plot from commercial software showing a colour map of deviation of measured point cloud data positions from that predicted by the CAD drawing

2 INDUSTRIAL OVERVIEW

As awareness of the benefits of XCT systems has increased, and additional distinct user applications identified, the demand for higher resolution and more accurate measurements has become apparent. This increase in the applications of XCT systems has initiated research into the worldwide markets for XCT scanners (see for example, [7]).

In its infancy XCT was a diagnostic tool, generally used in medical applications for the investigation of tumours in the human body. Today, there are film-based X-ray inspection systems, XCT inspection systems and computed radiography inspection systems. The market for such systems is growing and includes industries such as aerospace and defence, automotive, and energy and electronics. Sales of XCT systems were affected during the 2008 to 2009 peak of the current global financial crisis, but are recovering. It is estimated that the world market earned revenues for X-ray inspection systems in 2009 was $344 million and it is predicted that this will grow to $450 million in 2014 [8]. It is estimated that global installations of XCT scanners will reach 60 000 units by 2015 [9]. Industrial requirements can be subdivided into three trends, which will be discussed in section 2.1.

A survey produced by Frost & Sullivan [8], states that of the total X-ray inspection system market, the percentage of revenues by geographical region in 2009 was 32.2 % from North America, 27.5 % from Europe, 27.3 % from Asia Pacific and the remaining 13 % from the rest of the world.

The entire application of XCT for NDT has been enabled by medical funding and R&D as well as consumer camera and graphics cards development. The XCT NDT development path has been limited by progress in these industries.

2.1 CURRENT INDUSTRIAL TRENDS

Requirements for quality and safety have led the aerospace industry to maintain its position as the largest user of X-ray inspection systems through its use in NDT. However, disasters in the oil industry, such as that in the Gulf of Mexico, have led the oil and gas industry to have a more critical approach to the maintenance of its equipment. The oil and gas industry is also a user of XCT for on-site and field inspection, to estimate the viability of oil extraction. Emerging from the economic crisis, the automotive industry is also placing greater emphasis on improving the overall productivity and efficiency of manufacturing operations.

The digital age has had a crucial influence on the capture and analysis side of X-ray inspection techniques. Digital cameras have made the capture of images easier, the use of computers to analyse these images has made diagnostics more repeatable and the ability to generate 3D images has given the operator a different view on the data. Software packages have sufficiently simplified the acquisition and analysis of the images that these systems can now be operated by a non-specialist.

The profound economic, human and environmental impact of recent industrial disasters, such as the 2011 Fukushima nuclear plant incident in Japan, the 2010 BP fire and oil spill in the Gulf of Mexico, the 1984 Bhopal tragedy in India and 1988 Piper Alpha explosion in the North Sea, have led to increased pressure on industry to ensure that such catastrophes do not happen again. Cost-effective adherence to resultant regulation and legislation demands faster and more informative NDT systems. Specific inspection challenges include the optimisation of fracture identification and the accuracy of measurement of geometry of concealed parts, tasks for which XCT systems would be suitable.

2.2 EMERGING MARKETS

Demand for more sophisticated XCT systems is being driven by the fields and technologies in which the systems are finding growing applications. Examples of such fields and technologies include dual energy techniques, molecular characterisation of substances, slice scanners and positron emission scanners.

2.2.1 Food inspection

X-ray inspection systems are being used in the food industry for the detection and elimination of contaminants such as stone, glass, bone and plastic regardless of the type of packaging used. X-ray systems are generally integrated within the food packing system and typically inspect every can or package produced.

2.2.2 Security

The increased emphasis on security of transportation networks as a result of terrorist activity has ensured the introduction of so-called ‘full-body scanners’ at airports and other transport hubs. Such scanners are based on X-ray imaging technologies and facilitate detection of concealed narcotics, weapons and explosives. Additionally, X-ray detectors are used by immigration officials at border crossings to detect people purposely concealed within vehicles. There is also a great demand from port authorities to have X-ray equipment capable of examining 100 % of incoming containers. The limiting factor to container scan rate it is not the 20 s required to scan a container, but rather the time consumed by the operator interpretation of the images. Manufacturers, such as Rapiscan [10], are developing systems that do not output images for inspection but detect specific chemical elements, see also TEDDI [11]. Here neutrons create gamma radiation when they interact with the elements of the inspected object. These gamma-ray energies are unique to the atoms in the inspected object. If the gamma-ray signatures match those in a threat database, the system automatically sends out an alarm.

2.2.3 Microelectronics

X-rays inspection systems may be used in industry to characterise critical material properties of a wide variety of materials, such as gate materials, under development for the semiconductor industry. XCT systems are routinely used to examine electronic circuits to measure and verify that circuit tracks conform to their design criteria.

2.3 FUTURE MARKETS

Greater awareness of the capabilities of X-ray inspection technology and improvements to available diagnostic tools will result in broader application of the technology. Key potential markets for which X-ray inspection technologies are suitable, in principle, are discussed in this section.

2.3.1 New material technologies

NDT uses X-ray inspection technologies to facilitate the development and characterisation of new materials, such as semiconductors, superconductors and energy storage nanomaterials.

2.3.2 Military hardware

In general, national defence policies motivate and financially support a significant fraction of research and development. It is envisaged that X-ray inspection systems will become a routine tool in defensive military hardware.

2.3.3 Infrastructure

In 2010, American Science and Engineering, Inc [12], received an $8.2 million order to supply cargo inspection systems to secure critical infrastructure in the Middle East. The cargo inspection systems will be used to detect explosive threats and contraband concealed within vehicles entering high-risk facilities.

2.3.4 Industrial versus medical systems

Although technologies such as computed radiography (CR) and XCT are now becoming more mainstream in industrial application, their rate of adoption in emerging technologies is comparatively slow. Advances in the healthcare industry (see figure 7) may be used to predict the rate of adoption of such new technologies for industrial applications.

Performance specifications for X-ray inspection systems are highest for metrology, with a less stringent requirement for industrial applications and less again for medical applications.

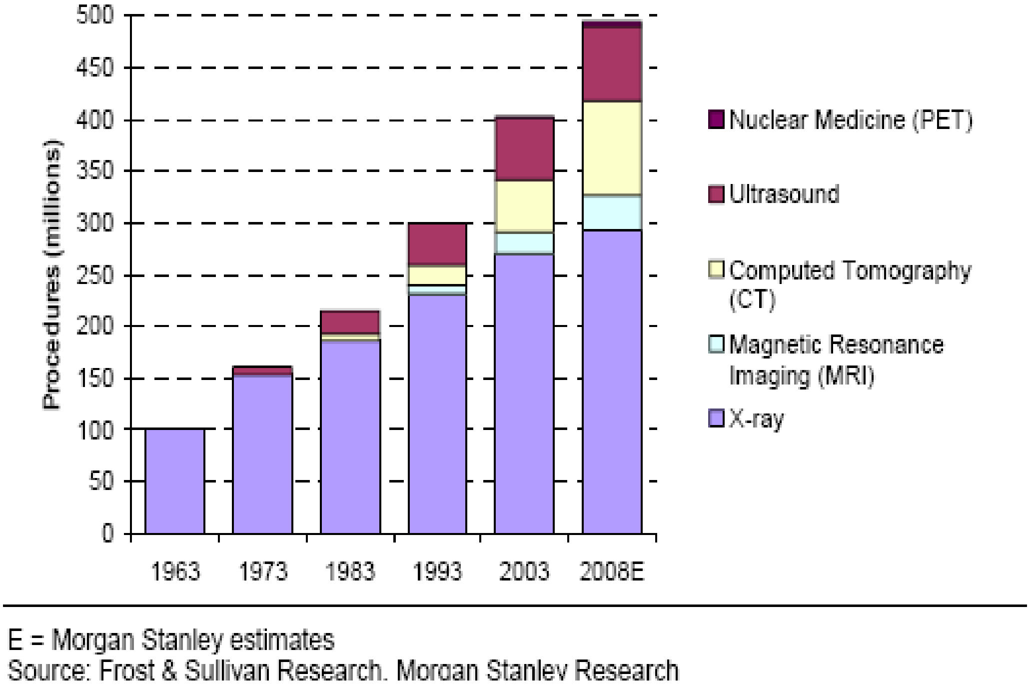

Figure 7. Imaging trends: diagnostic imaging procedure volume by modality [8]

2.3.5 Aerospace demands

Aerospace applications account for about 25 % of the X-ray inspection market. These applications can be grouped into two categories: flaw detection and dimensional metrology. Flaws to be detected include cracks, inclusions and voids. Dimensional metrology is used to compare fabricated components with their original design requirements, to determine:

- whether variation in the manufacturing process introduces significant changes to the final products;
- to what extent the final part represents the part envisaged by the designer;
- whether the limit of wear on parts conforms to what is deemed acceptable; and
- the optimum service period for a given designed component, with greater accuracy.

2.3.6 Electronics demands

Use of X-ray systems in the electronics industry is growing and such systems have now become the most widely used tool for the quality control of products such as printed circuit boards (PCBs), integrated circuits (ICs) and high-density ball grid array (BGA) chips. For this industry, the main use of X-ray inspection is the detection of flaws such as solder fracture, voiding and bridging, with metrology currently a lower priority.

3 XCT HARDWARE

The correct design of the hardware of an XCT system is critical to its ultimate performance. Further, an understanding of the constituent parts is essential for an appropriate uncertainty analysis. The following areas of hardware specific to XCT will be the focus of this section.

- X-ray source.
- Detector.
- Computer.
- Shielding.
- Cooling system.

Sub-systems, such as the manipulation system, vibration isolation, power supply and environmental control are of wide-spread and long-standing concern to precision dimensional metrology and have been addressed in detail elsewhere [13-16]. Consequently, they will not be discussed in detail in this report.

3.1 X-RAY SOURCE

The discovery of X-rays is usually credited to the German physicist Wilhelm Röntgen as he was the first to systematically study them. He is also responsible for naming them, as in German, they are referred to as *Röntgen Strahlen*.

It is believed that the first discovery of X-rays was during the use of Crookes tubes in 1895 when it was realised that the photographic plates were being blackened; for a general introduction, see [17]. Use of the Crookes tube, invented twenty years previously and related to modern cathode ray tube display technology, also led to the formal identification of electrons [18].

X-rays are produced by accelerating electrons through a high voltage, in a vacuum tube, and allowing the electrons to collide with a metal target. X-rays are produced through two distinct processes: bremsstrahlung and characteristic radiation.

Bremsstrahlung, or ‘braking radiation’, is caused when an electron approaches very close to the nucleus of an atom, but does not actually collide with any part of it. During this process, the electron is affected by the strong nuclear attraction, where the positive charged nucleus attracts the negatively charged electron. The resulting loss in energy, due to the interaction, leads to the emission as a photon with the same energy. This sudden deceleration of the electron gives rise to the radiation known as bremsstrahlung. The probability of this type of radiation increases with the target’s atomic number (Z) and with increasing energy of the electrons. The spectrum of bremsstrahlung X-rays is continuous.

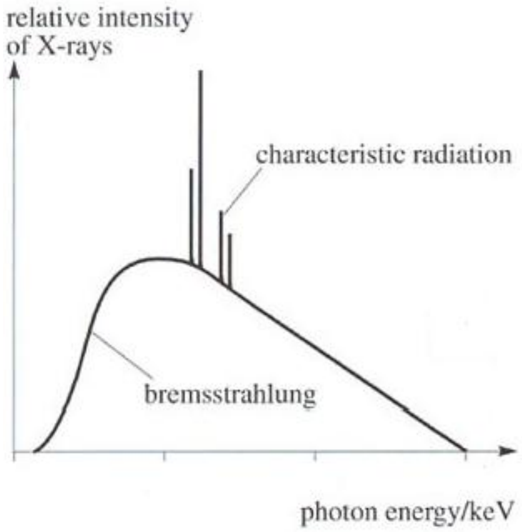

Figure 8. X-ray spectrum

Characteristic radiation is caused when the incoming electron collides directly with one of the shell electrons, creating an electron vacancy. When this vacancy is filled with an electron from an outer shell, a discrete spectrum of X-rays is emitted. Characteristic radiation, depending on the atomic number of the target, produces energy spikes that are superimposed onto the bremsstrahlung radiation (refer to figure 8). These characteristic X-rays are a property of the target material. As the wavelength of the X-rays used is decreased, the energy per photon increases, along with the capability for higher spatial resolving powers (see [19] for a more thorough analysis).

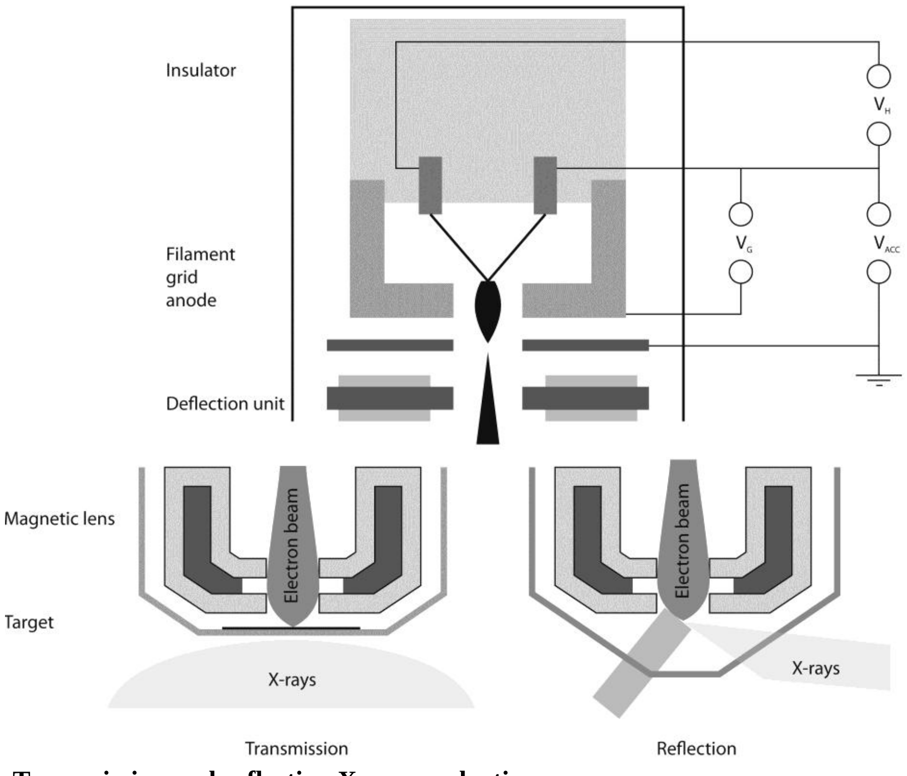

Figure 9. Transmission and reflection X-ray production

Depending on the direction of the X-rays produced, X-ray tubes can be categorised into directional and panoramic tubes. Based on the way the electrical earth is arranged relative to the anode and the cathode, X-ray tubes can be divided into unipolar and bipolar X-ray tubes [20]. The bipolar tube design can operate at voltages up to 450 kV, whereas the unipolar tube design can only operate up to 300 kV.

The structure of an X-ray tube is shown in figure 9, where the main parts are a filament (cathode) and a target (anode). To avoid interaction with molecules of the gas that can produce lower energy secondary electrons, the X-ray radiation requires a vacuum environment. The conventional design utilises a sealed evacuated glass tube, whereas metal and ceramic tubes are increasingly used nowadays due to longer tube life expectancy and higher heat capacity. It is also common to use open tube designs, where the tube is only evacuated when powered up [21]. The benefit of using an open tube design is that failed parts, for example, a burnt target, can be easily changed and the tube can be cleaned and maintained from time to time. The open tube design is often used in high resolution XCT systems.

The cathode consists of a thin filament (usually tungsten) and the anode contains a small amount of a tungsten, molybdenum or copper target, which has a high melting point. The anode is also embedded in to a relatively large amount of copper [22], where the copper helps to disperse the heat generated. When the X-ray tube is powered up, electrons are produced by thermionic emission from the electrical heating of a filament. These free electrons are accelerated towards the anode due to the electric potential. When the electrons hit the anode, they collide with the atoms of a target object producing X-rays. If the target material is thin enough, and the electron energy high enough, then X-ray photons are transmitted through the target. The process is the so called transmission type of X-ray production. However, if the target is sufficiently thick and the electron energy is sufficiently low, then the X-rays are emitted in a manner imitating reflection, which is the reflection type of X-ray production.

When the X-ray tube is working, approximately 1 % of the energy generated is emitted as X-rays and the remaining energy is released as heat. The significant amount of heat generated can produce damage and can affect the stability of the X-rays generated. Modern designs use rotating anode tubes so that heat can be dispersed on different parts of the target plate. Apart from using rotating anode and copper for heat dispersion, recirculating systems of water, oil or other thermal conductive materials are often used to cool X-ray tubes.

The output X-rays usually pass through a circular aperture or diaphragm (for cone beam) or through collimating plates (for fan beam) [23].

The focal spot size is important in determining the image quality. Conventional XCT systems have a focal spot of larger than 1 mm. Microfocus systems have a spot size of between 1 µm to 1000 µm [23] and nanofocus systems have a spot size of less than 1 µm [24, 25]. Generally speaking, focal spot size is smaller when lower power is applied. However, with lower power, the ability for imaging is limited.

The voltage and the current supplied to an X-ray tube are important parameters for controlling the X-rays that are produced. The voltage (usually in kilovolts), determines the X-ray spectrum [20]. Increasing the voltage effectively decreases the wavelength of the X-rays emitted [26] and increasing the current at constant voltage increases the X-ray intensity without changing the X-ray spectrum.

3.2 X-RAY DETECTORS

As discussed above, the first evidence for X-rays was found unexpectedly by exposing photographic plates. However, Röntgen also noticed that a barium cyanide coated screen, stored in the vicinity of the experiment, glowed when the apparatus was energised and ceased to glow when the apparatus was switched off - this was probably the first encounter with X-ray scintillation. There have been several papers investigating the accuracy and reliability of X-ray detectors, for example [27]. Figure 10 outlines the advances in detectors over the last forty years [28], where the sensitivity and dynamic range increase significantly.

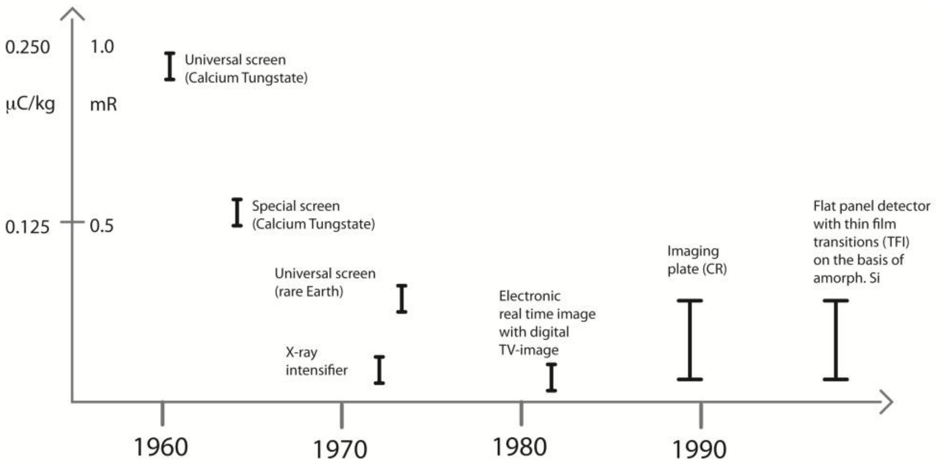

Figure 10. Advances in detector technology [28]

There are many different types of X-ray detectors. ISO 15708 part 1 [29] splits X-ray detectors into two groups: ionization detectors and scintillation detectors. More information about different types of detectors is given in [30], for example, semiconductor detectors and CCD detectors.

- **Direct semiconductor detectors**

As photographic detectors have evolved, their use in the detection of radiation, both in the optical and X-ray frequency range, has become commonplace. Semiconductor detectors, using silicon or germanium doped with lithium, have been around since the 1970s. These devices produce an electrical current when exposed to X-rays and are generally referred to as solid state detectors or direct detectors (see figure 11). Some modern direct detectors use photoconductors, such as amorphous selenium or cadmium telluride coatings on a multi-pixel microelectronic plate, and the output current is collected by an array of thin film transistors (TFTs). Currently available systems on the market, such as the FT50m detector [31], manufactured by Teledyne Dalsa, have claimed pixel size of 5.6 µm × 5.6 µm.

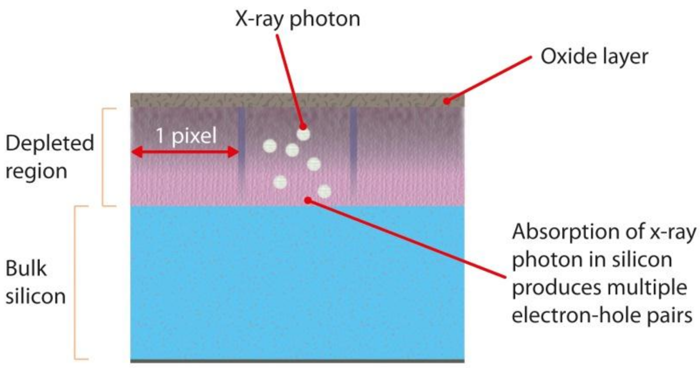

Figure 11. Direct detection of X-ray photons

Direct detection is beneficial due to the increased sensitivity. The detector acts as a single photon counter. When flux levels are low and a single photon is acting on a single pixel, direct detection makes it possible to resolve the energies of the incident photons using the number of counts generated from the detector. This method is known as energy dispersive X-ray spectroscopy. However, when the photon energy is high (greater than 20 keV), the photon passes straight through the detector without any interaction between the detector and the photon. Overexposure to X-rays may also damage the CCD. This can manifest itself as an increase in dark current [32] and a voltage shift of the sensor. Sensors are generally small in area, for example 25 mm × 25 mm; cost increases dramatically with size. To reduce shot noise, detectors are sometimes cooled using liquid nitrogen, Peltier cooling or other methods.

- **Scintillation detectors**

In general, scintillation is a flash of visible light produced in a transparent material by an ionisation event. Scintillation detectors can convert high-energy X-ray photons into lower energy photons in the visible wavelength range, and these optical photons can then be detected by means of a photomultiplier tube or a photodiode. Scintillation detectors use this principle, and have the advantage that they are more sensitive to lower doses of X-rays.

A scintillator and a flat panel detector (FPD) together form an indirect FPD. The scintillator coating converts the X-rays to visible light and the photo diode or photomultiplier tube then converts the visible light to a digital output. Hence, this type of detector is also termed an ‘indirect’ detector. Typical materials used for indirect FPDs would be sodium-activated caesium iodide on a substrate of an amorphous silicon detector (see figure 12).

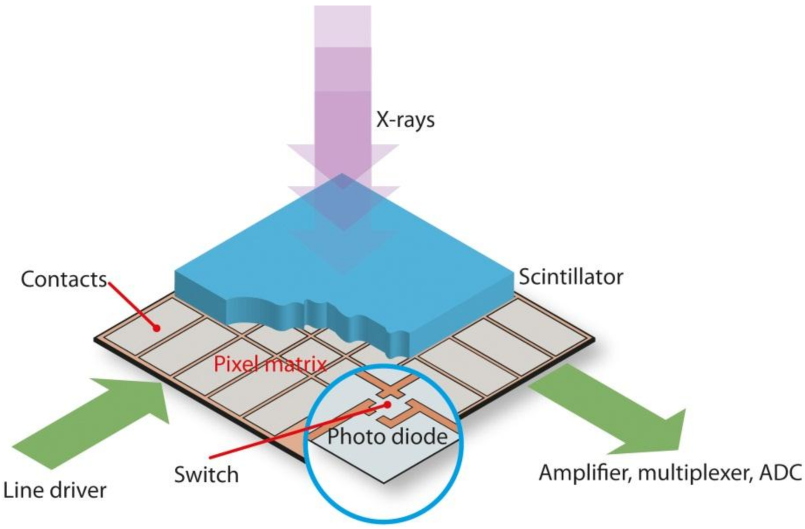

Figure 12. Structure of a scintillation detector [28]

3.3 PROPERTIES OF XCT DETECTORS

The most important detector characteristics are: field coverage, geometrical characteristics, quantum efficiency, sensitivity, spatial resolution, noise characteristics, dynamic range, uniformity, acquisition speed, frame rate and cost [33].

- **Field coverage**

If parts of the object under examination are not detected at every position, there will be an error in the final computation that cannot be determined. This lack of information causes errors in XCT scanning – see section 5.4 for more details.

- **Geometrical characteristics**

Due to the presence of sensor circuitry adjacent to each pixel, a small but significant, fraction of the display area is insensitive to incoming radiation. This area is referred to as the ‘dead’ region and is not used in analysis. Distortion due to non-uniform scaling is also considered as one factor that can affect the geometrical characteristics of X-ray detectors.

- **Quantum efficiency**

In all X-ray systems, the radiation must interact with the detector in some manner that will produce a signal that is useful. The probability η that an X-ray photon will interact with the detector is given by the equation (1)

$$\eta = 1 - \exp\left(-\mu\left(E\right)T\right) \tag{1}$$

where T is thickness of the detector, $\mu(E)$ is the linear attenuation of the detector and E is the energy of the photon (a function of the photon frequency) [33]. As the beam passes through an object, the beam is hardened due to the absorption of the lower energy photons and the remaining high-energy photons now have a greater efficiency on the detector. It is for this reason that the efficiency of the detector should be calibrated over a range, or spectrum, of frequencies. The efficiency of the detector is directly proportional to the thickness of the detector, or more accurately the thickness of the active zone of the pixel. If two pixels are of different thickness they will have different efficiencies. Detection of the beam is reliant on the photon interacting with the nucleus of the material in the detector, therefore, the further through the material that the beam has to travel the greater the probability of interacting with at least one atomic nucleus.

- **Sensitivity**

The sensitivity of a measuring system is described in VIM [34] as the quotient of the change in an indication of a measuring system and the corresponding change in a value of a quantity being measured. By using statistical methods and filtering, the sensitivity of a detector can be increased. However, manipulating the raw data in this way may cause useful information to be discarded.

- **Spatial resolution**

There are many factors in XCT systems that influence the spatial resolution of the system: the focal spot size of the X-ray source, the performance of the detector, the magnification of the system, the number of projections, the reconstruction algorithms used, and any applied filtering. The term spatial resolution will be discussed further in section 6.4.1.

- **Noise**

Any image generated by an XCT system will contain a certain amount of noise, for example, noise may be due to the detector, beam profile variation, or some other system parameter variation. However, it is assumed that this noise is centred on a fixed mean value and that this mean value may be predicted with a reduced uncertainty by reducing the size of this noise [35]. The noise power is inversely proportional to the number of scans taken, for a given constant intensity per scan [36].

- **Dynamic range**

In general, a photo-detector will only have a linear response over a finite range of input signal energy. Outside this range it may become non-linear or provide no response at all. In the case of an X-ray detector, when the photon energy is too low, it may not have sufficient energy to displace an electron. Equally, if there were insufficient photons, then the probability of any collision occurring would be extremely small. Even when the photons have sufficient energy and number to generate a signal, this signal may be lost in the noise. The lower level of this input that cannot be discriminated from the detector noise is termed the noise equivalent input.

At the other end of the scale, for the case where the energy of the photon is high and the number of photons large, the detector may be unable to discriminate between two adjacent photons, resulting in a saturation effect known as blooming. In some cases the dynamic range of a detector is related to the signal-to-noise ratio, which is equal to the ratio of the average signal intensity over the standard deviation of the noise.

- **Uniformity**

Uniformity describes the variation of response to a constant, spatially uniform incident X-ray illumination across the face of the total receptor area. Areas where the detector does not have the same sensitivity can be corrected for in software, generally by using a look-up table derived from a characterisation of the detector.

- **Capture duration**

There are many individual parts that contribute to the capture and processing of the data for XCT systems. Measuring volume, resolution and speed of processing are some examples. Currently, objects as large as automobile cylinder heads can be scanned, using medical XCT systems in a few minutes with a resolution on the order of 100 µm. On an industrial XCT system, the scan can take ten to twenty hours with a resolution of a few micrometres.

- **Weight limit**

As a general rule, if the measuring volume of an XCT increases, so too does the weight carrying capability. However, XCT systems rely on the relative absorption of the photons - if all the X-ray photons are absorbed before reaching the detector then there are no data for analysis. Materials with high atomic number are more efficient absorbers of X-ray photons. The largest volume that can be measured is that volume that allows sufficient X-ray photons to reach the detector, to allow a confident analysis. As different materials have different densities, this means that the maximum volume of the object is dependent on the object's density.

3.4 PC HARDWARE

After the images have been acquired from the detector for each of the rotational positions, the set of images are passed through a series of computations that translate this information into voxels. The process can be time-consuming and requires a lot of computing power. Hence, the capability of the computer is critical. Generally, three components have to be considered when building a computer for XCT data reconstruction and data analyses. These components are central processing unit (CPU), random-access memory (RAM) and graphic cards. Recent development in multi-core processors and advanced graphic cards with graphics processing units (GPUs) can significantly accelerate the speed when handling large amounts of data and increase speed of image decoding. The flexibility for the user to choose a suitable size of computer memory allows large amounts of data to be read. At the time of writing, it is common to use a computer with 96 gigabyte of RAM in the computers for XCT systems. It is believed that this figure will be dramatically increased shortly. It is also noticed that super-computing power is expensive. However, the development of grid computing offers other chances to significantly improve the efficiency of data analyses, where the cost can be shared between a few users.

3.5 SHIELDING

Health and safety is important when operating an XCT system. Critical parameters, such as beam power, workload, scatter and leakage, must be taken into account when calculating the required shielding [37]. The traditional material used in the shielding of harmful X-rays is lead, due to its high density (11340 kg m^{-3}) and atomic number (82). As the energy of the X-ray beam increases then the resultant thickness of the shielding needs to be increased.

3.6 COOLING SYSTEM

Because of the low efficiency of the X-ray production process, XCT systems, especially systems generating high power, require cooling systems due to the amount of heat dissipated by the target. By keeping the system at a fixed temperature, the instability of the system through thermal effects may be greatly reduced. By cooling the detector, the signal-to-noise ratio may also be increased. As discussed in section 3.1, the cooling of an X-ray tube is critical in XCT systems. However, an external cooling system is also important to maintain temperature stability in the measurement chamber. More detailed information regarding cooling can be found elsewhere [38-41].

4 DATA PROCESSING

Data processing plays an important role in XCT technology. Without the reconstruction process, the XCT images are simply radiographs as provided by conventional radiology. This section reviews the data reconstruction process and the software available on the market.

Assuming an XCT system with a detector of $M \times N$ pixels and P projections with different rotation angles has been taken for one measurement, the reconstruction process involves solving an $M \times N \times P$ cubic matrix of attenuation coefficients (see figure 13).

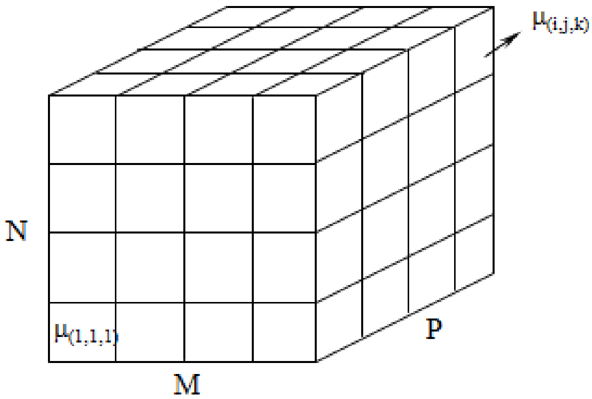

Figure 13. XCT cubic matrix of attenuation coefficients

For XCT systems, the X-ray beam penetrates the sample and projects on to the detector. The resultant radiography image is the projection of the sample and the intensity of each pixel is a function of the attenuation coefficient and the distance the X-ray travels within the sample. The projection can be calculated using a Radon transforms, see equation (2) [42], where the Radon transform of a ray passing through a medium $f(\boldsymbol{x})$ with length L is the line integral and projection is given by

$$pf(L) = \int_L f(\mathbf{x})|d\mathbf{x}| \quad \textbf{(2)}$$

The task of XCT reconstruction is to find $f(\mathbf{x})$ given a knowledge of $pf(L)$. This process is called backprojection, which can be solved using an inverse Radon transform.

The Radon transform and its inverse function form the mathematical basis for reconstructing tomographic images from the projection data. The images in figure 14 and figure 15 illustrate the Radon transform and inverse Radon transform of the image of a square object. However, the backprojection based on an inverse Radon transform process results in a blurred image. This can be minimised by applying a filtering process before backprojection (see figure 15).

The filtering used in the reconstruction is generally a low pass filter type. There are many filters that can be used for reconstruction purposes. Examples include the Shepp-Logan, Laks, Ramachandran and Ramp filters [43-45]. Some typical filters are presented in figure 16.

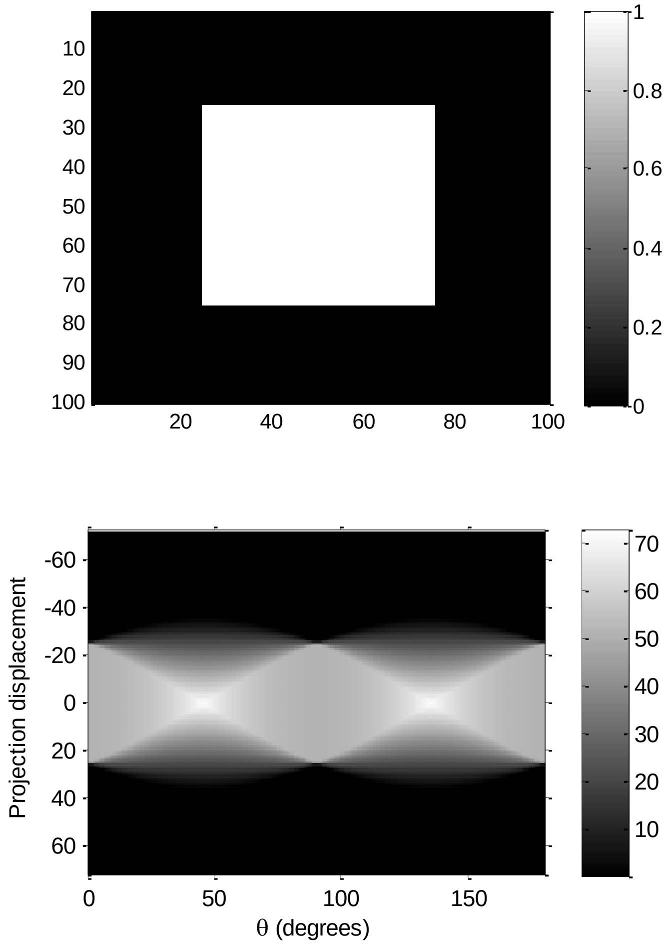

Figure 14. Illustration of Radon transform for a square object (top) image of a square (bottom) Radon transform of the square image from 0° to 180°

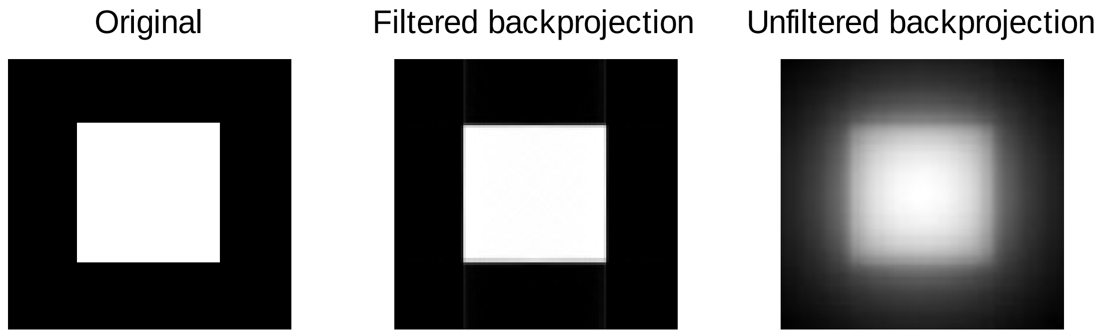

Figure 15. Inverse of Radon transform (left) original square image (middle) image reconstructed using filtered backprojection process (right) image calculated using unfiltered backprojection process

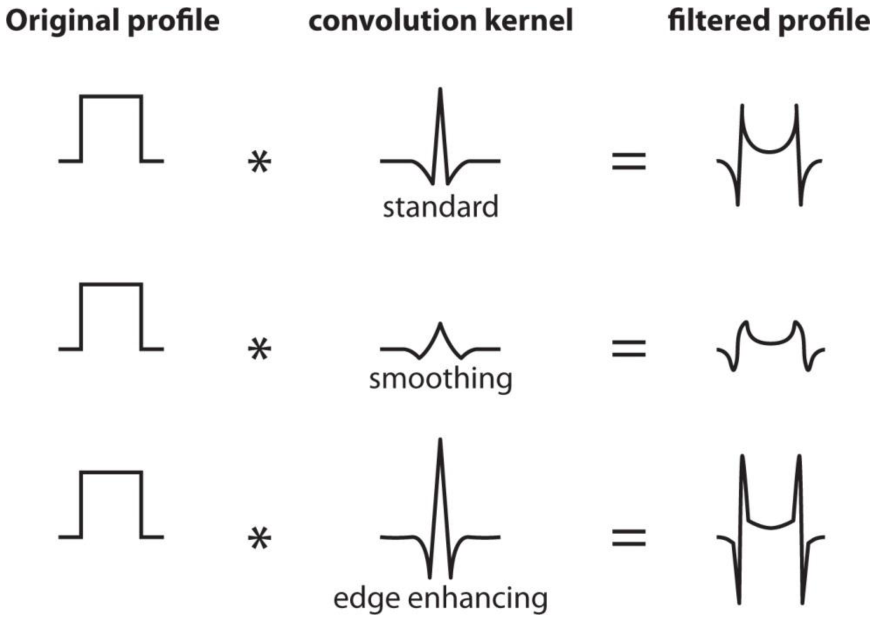

Figure 16. Operation of typical filters [46]

Given the potential benefits, it is common to filter the projection data before applying the backprojection process. However, variants exist where the backprojection is performed before the filtering procedure. Filtered backprojection algorithms are more accurate than the image reconstructed by backprojection filtering algorithms. The differences resulting from this change in processing order is discussed elsewhere [47].

4.1 RECONSTRUCTION OF CONE-BEAM XCT

Many researchers have considered the reconstruction of cone-beam data. Key algorithms are compared in [48] (and see table 2). The following discussion is based on the algorithms listed in table 2.

There are a number of aspects that should be considered when evaluating different reconstruction algorithms. The first aspect is whether the algorithm is exact or non-exact. An exact algorithm is mathematically correct if the data are noise-free and captured with sufficient density along the source trajectory with a detector array having sufficient detector element density. Non-exact algorithms are more flexible in the case where there are missing data points or there are insufficient projection data in a given angular interval [49]. The geometry (trajectory or path) of the X-ray vertex point is also important. The term vertex point refers to the position of the X-ray source [50]. Smith [48] concluded that one scan has complete information about an object if, on every plane that intersects the object, there lies a vertex. For example, vertex geometries of two periods of a sinusoid on a cylinder provide complete information about an object. However, the implementation of scan with complex vertex geometry can be poor. For example, the method developed in reference [51], which requires a sphere vertex geometry, is difficult to achieve in practice. Apart from those aspects considered above, the implementation and efficiency of those algorithms have been considered in table 2.

The two main categories of algorithms are ‘analytic’ and ‘algebraic’, where algebraic algorithms demand more computing power than analytic algorithms. Thus, due to high reconstruction speed, the analytic algorithms are more efficient in practice [52]. Convolution backprojection, matrix inversion and Fourier transform are analytic algorithms. The algebraic reconstruction technique (ART), simultaneous iterative reconstruction technique (SIRT) and iterative least-squares technique (LST) are algebraic methods.

Table 2. Comparison of reconstruction algorithms [48]

Researcher	Exact/ Non-exact	Implemented	Computing efficiency	Geometry of X-ray vertices	Reconstruction method
Altschuler	N	No	Fair	Circle	Matrix inversion
Feldkamp [5]	N	Yes	Excellent	Circle	Convolution backprojection
Finch [53]	E	No	n/a	Sufficiently large circle	A mathematical analysis
Grangeat	N	Yes	Good	Circle	Convolution backprojection
Hamaker [54]	N	No	Fair	Finite number of sources	Convolution backprojection
Herman [55]	N	Yes	Excellent	Circle	Convolution backprojection
Imiya [51]	N	Yes	Poor	Sphere	Rho-filter convolution backprojection
Kowalski [56]	N	Yes	Fair	Two parallel circles	Matrix inversion
Kowalski [57]	N	Yes	Fair	Straight line	Matrix inversion
Minerbo [58]	N	No	Fair	Circle	Convolution backprojection
Peyrin [59]	N	No	Poor	Sphere	Rho-filter convolution backprojection
Schlindwein [60]	N	Yes	Fair	Two parallel circles	Algebraic reconstruction technique
Smith [61]	E	No	Poor	Sphere	Convolution backprojection
Tuy [62]	E	No	Poor	Two perpendicul ar circles	Convolution backprojection

Currently, convolution backprojection is the most popular method in XCT reconstruction. The most popular and efficient solution for cone-beam flat panel detectors was developed by Feldkamp [5]. The algorithm was adapted from the fan beam algorithm based on an assumption that the vertex geometry of an X-ray source is a circle. The reconstruction of a cone-beam source with a cylindrical detector is discussed in [49]. A circular cone beam CT reconstruction is presented elsewhere [63].

Most XCT manufacturers develop proprietary reconstruction software. For example, Nikon provides *CT pro* [64] and GE provides *phoenix datos|x* [65] to reconstruct data. The most common reconstruction algorithm used in practice is the filtered backprojection algorithm.

4.2 COMMERCIAL VISUALISATION SOFTWARE PACKAGES

There are a number of commercial software packages available for volumetric visualisation of reconstructed XCT data. Most of these packages provide basic functions such as visualisation and segmentation. Some brief information on these software packages is provided in this section.

VGStudio MAX was developed by Volume Graphics for the visualization and analysis of XCT data. The company was founded in 1997 in Heidelberg, Germany. Four add-on modules are available for end-users. These modules are "Coordinate Measurement", "Nominal/Actual Comparison", "Porosity/Inclusion Analysis" and "Wall Thickness Analysis".
Website: www.volumegraphics.com/ Accessed on 1st August 2011

Avizo is a commercial software package that is available to visualise volumetric data. Its predecessor was Amira and it was originally developed by Visualization and Data Analysis Group. Avizo has been commercially developed and distributed by Visualization Sciences Group. The software also has four extension modules designed for different purposes. These are Avizo Earth for geosciences and the oil and gas industries, Avizo Wind for simulation data, Avizo Fire for materials science and Avizo Green for environmental data.
Website: www.vsg3d.com/ Accessed on 1st August 2011

Simpleware is a volumetric data processing software package with a focus on converting volumetric data into CAD and finite element models. Simpleware was developed by Simpleware Ltd., a privately owned company based in Exeter, UK. The core software is ScanIP, in which the user can segment and export the data. Simpleware has two extended modules, ScanCAD for mesh generation and ScanFE for CAD integration.
Website: www.simpleware.com/ Accessed on 1st August 2011

4.3 FREEWARE

Apart from commercial software, there are also many freeware packages available over the Internet. Many of the freeware packages are capable of running on multiple software platforms and the source code is freely available to end-users.

Drishiti was developed by Ajay Limaye at the Australian National University. The software offers many useful visualisation features for volumetric data.
Website: anusf.anu.edu.au/Vizlab/drishti/index.shtml Accessed on 1st August 2011

VolPack was developed by Philippe Lacroute at the Stanford Computer Graphics Laboratory. The software was based on a family of fast volume rendering algorithms [66]. The library is intended for use in C or C++ programs.
Website: graphics.stanford.edu/software/volpack/ Accessed on 1st August 2011

ImageJ was developed by Wayne Rasband at the National Institutes of Health in United States. It was written in Java and the source code is free and in the public domain. The software offers users simple solutions to calculate area and pixel values of user-defined selections. It can also calculate distances and angles and provides plugins such as filters and segmentation for advanced users.
Website: rsbweb.nih.gov/ij/index.html Accessed on 1st August 2011

Visualization Toolkit (VTK) is an open-source software system for volumetric computer graphics, imaging processing and visualization. It utilises a C++ class library and interpreted interface layers including Java and Python. VTK supports many features such as polygon reduction, mesh smoothing and parallel processing.
Website: www.vtk.org/ Accessed on 1st August 2011

Paraview is an open-source, multi-platform software for visualization and data analyses, developed by Sandia National Laboratories, in conjunction with NVIDIA Corporation and Kitware Inc. As it uses distributed memory computing resources, the software is capable of parallel rendering and can be used to process very large datasets.
Website: www.paraview.org/ Accessed on 1st August 2011

5 SYSTEMATIC ERRORS IN XCT

There are many sources of systematic error related to XCT technologies. These errors have been reviewed previously [23, 67]. The most common systematic errors are reviewed in this section, for example, the errors related to the X-ray tube, the detector and the physical characteristic of XCT systems. Errors related to the setup of the sample are also briefly discussed.

The definition of the term ‘artefact’ used in the following is given in ISO 15708 part 1 [29] as: the discrepancy between the actual value of some physical property of an object and the map of that property generated by a XCT imaging process.

5.1 BEAM DRIFT

The accuracy of an XCT system can be significantly influenced by the spatial stability of the X-ray focal spot, that is, the presence of beam drift. The X-ray beam drift issue is related to the thermal expansion of the X-ray tube. The structure of a typical X-ray tube is illustrated in figure 9 and a more detailed schema of a reflection X-ray tube configuration can be seen in figure 17. When electrons hit the target and X-ray photons are emitted, a large amount of heat is generated. The temperature in the X-ray chamber can rise quickly within a very short period of time; indeed, damage can be caused if the temperature exceeds a critical level [38]. The dimensions of an X-ray tube can vary significantly due to thermal expansion in the presence of the excess heat load, resulting in the drift of the focal spot. This issue has been discussed in detail elsewhere [68, 69]. The current industrial solution is to integrate the cooling system inside the X-ray tube while maintain the system cooling unit [41] in the measurement chamber in order to improve the thermal control characteristics of the cooling system.

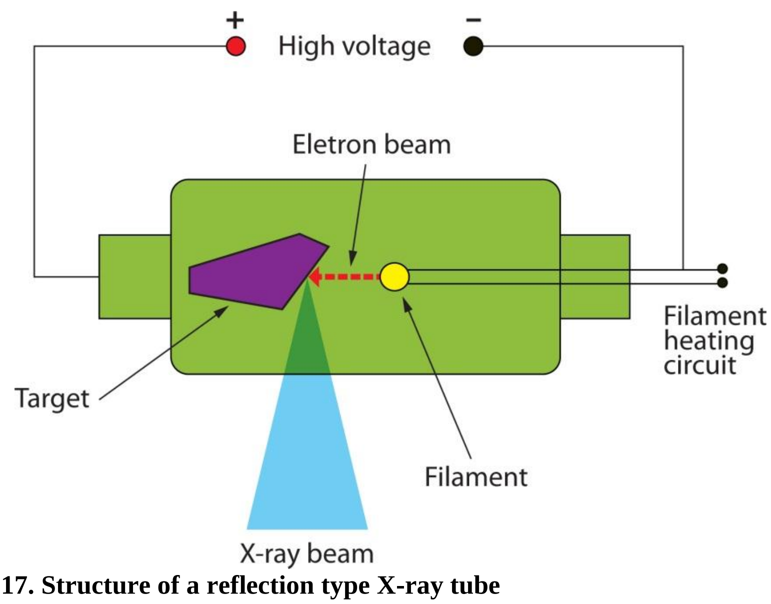

Figure 17. Structure of a reflection type X-ray tube

5.2 RING ARTEFACTS

Ring artefacts are a common issue related to XCT images. Such artefacts may be the result of defects in, or poor calibration of, detectors, non-linear behaviour of detector materials, channel to channel variation of the detector array output, *i.e.* poor uniformity, or mechanical misalignment between the X-ray source and the detector (see figure 18). Also, ring artefacts may be caused by the finite sensitivity of the detector. Among many detector properties discussed in section 3.3, sensitivity of the detector plays an important role. It is important to have a constant sensitivity across the whole detector [33]. If a pixel on the detector is faulty, the resulting images of the reconstructed volumetric data show a ring-like artefact.

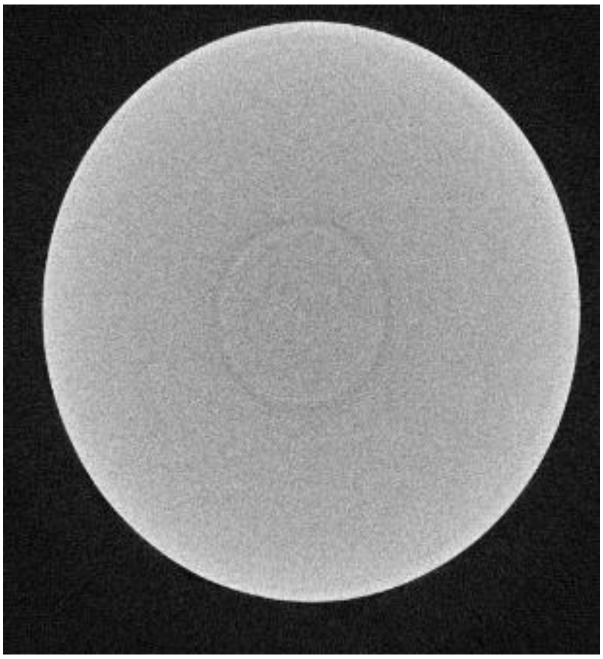

Figure 18. Illustration of ring artefacts (courtesy Nikon Metrology)

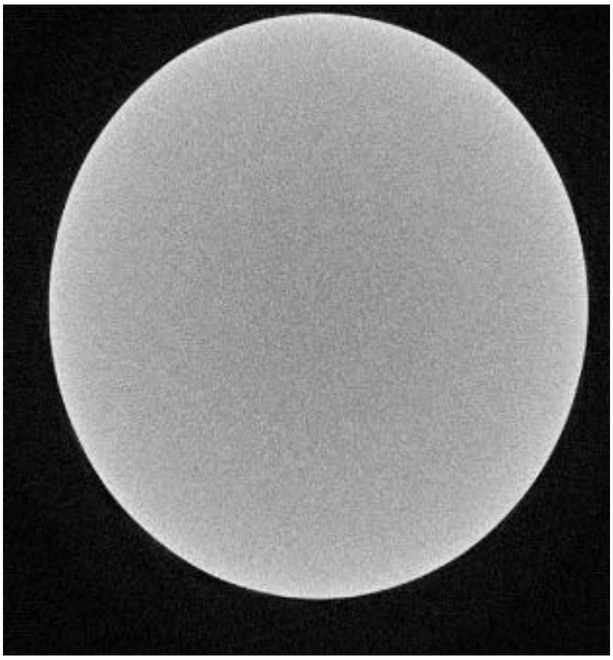

Figure 19. Image of ring artefact removed (courtesy Nikon Metrology)

Ring artefacts can be reduced by detector calibration if there is no permanent damage to the detector. The calibration of the detector is discussed in section 6.1. Ring artefacts can also be corrected numerically. This can be achieved by transforming the original XCT images from a Cartesian coordinate system to a polar coordinate system, whereupon the ring artefacts become a line and can be removed [70]. Figure 18 shows an image with ring artefacts and figure 19 shows the image with the ring artefacts removed.

5.3 BEAM HARDENING

Beam hardening is a phenomenon that is associated with a polychromatic X-ray beam. When X-rays travel through a dense material, the X-rays with lower energy are absorbed preferentially to those X-rays with higher energy levels (see figure 20). However, the XCT reconstruction algorithm works on an assumption that the absorption of the X-rays is a property of the material and is independent of the energy level of the X-ray photons. This mismatch between the assumption and the reality results in errors in the estimation of the attenuation coefficient of the material. Typical errors are as shown in figure 21, where in the reconstructed image the edge of the object is brighter than the interior.

The methods used to correct beam hardening effect can be divided into three types: pre-processing methods, post-processing methods and the dual energy method [71]. In practice, a physical filter can be used to pre-filter the source to remove low energy X-rays. The filter can be a thin plate of copper or aluminium, which can be placed between the X-ray source and the sample. This filtering method is straightforward to achieve in practice, but the method reduces the signal-to-noise ratio. Numerical correction of the beam hardening effect is discussed elsewhere [71-75]. It is suggested to use second and third order polynomial approximation methods [74] and iterative methods [71, 73, 75] to correct such an effect. The dual energy method is a method for producing images with different contrast characteristics to common X-ray images [76], where those images are taken using two X-ray beams to calculate the complete energy dependency needed for beam hardening correction [77]. Therefore, the dual energy process is time-consuming and expensive.

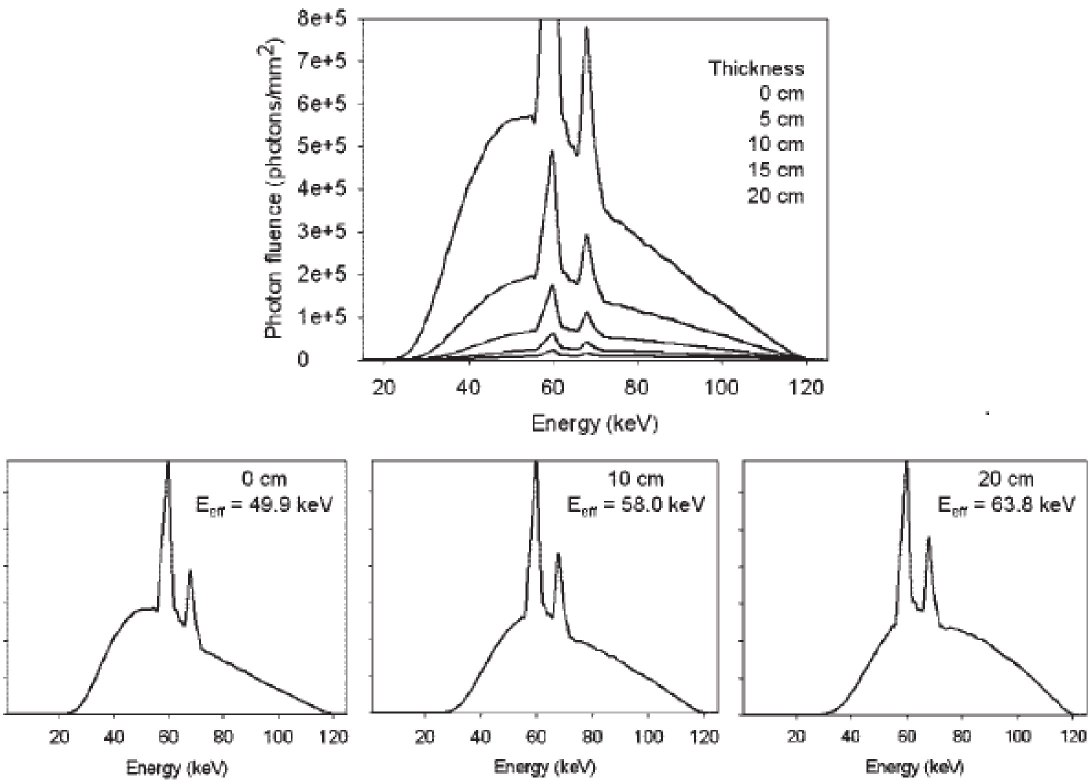

Figure 20. Illustration of X-ray penetrating sample with different thickness [78]

Two common artefacts resulting from beam hardening effects are ‘streak’ artefacts and ‘cupping’ artefacts [67].

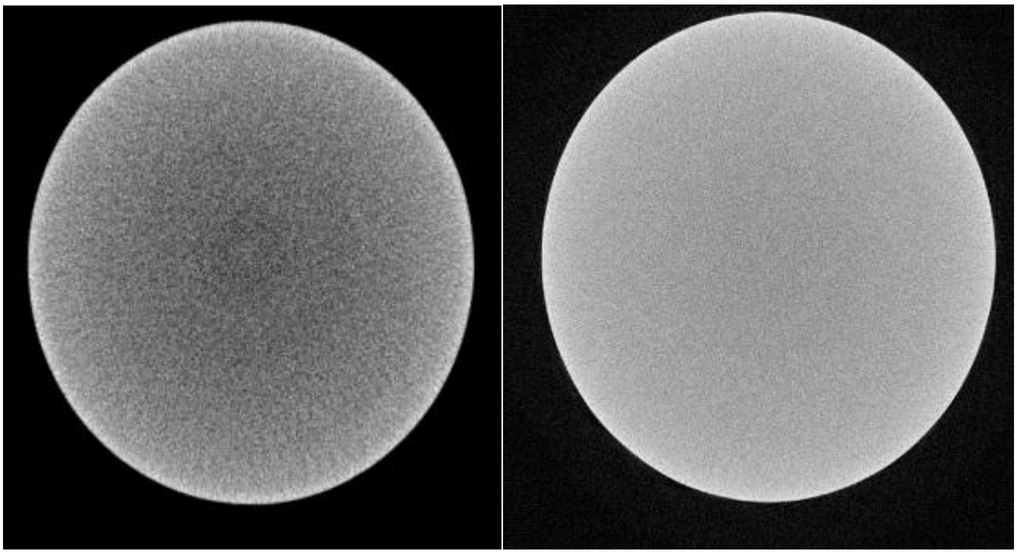

Figure 21. Beam hardening effects (left) an image without filtering (right) an image with a 1 mm thick copper filter (courtesy Nikon Metrology)

An example of streak artefacts can be seen in figure 22. Streak (or metal) artefacts are common in XCT images with typical black and white lines, which cause significant degradation in the X-ray image. Streak artefacts can be caused by many factors. For example, a sample with high-density metal parts can attenuate part or all X-ray energies, which leads to incorrect measurements of the objects behind the metal part. This can be corrected by raising the energy level of the X-ray source [79]. Streak artefacts can also be caused if the object is moved during measurement, insufficient rotational sampling points are specified, or if the instrument coordinate system is misaligned [80]. Streak artefacts can be corrected using a linearization technique based on a physical model [81].

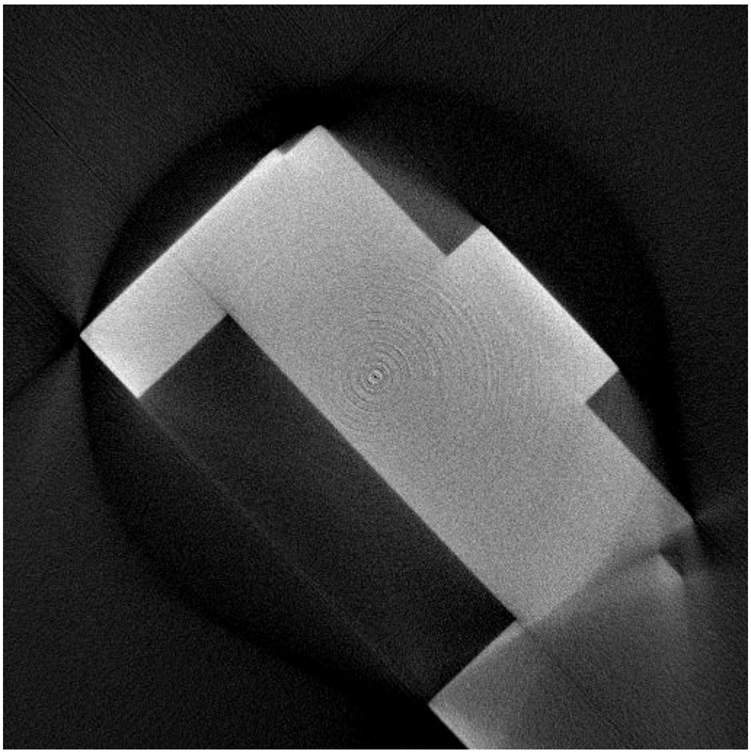

Figure 22. Illustration of ring artefacts and streak artefacts

Cupping artefacts are typically due to uncorrected beam hardening and scatter, in which the XCT density values in the interior of an object are reduced compared to those near the outside [29]. When X-rays pass through a cylinder of the same density, they harden in proportion to the amount of material they travel through. This means that the beams that travel through the centre of the cylinder are hardened more than those that pass through the edge of the cylinder (see figure 23). Cupping artefacts can be removed numerically and different methods are introduced elsewhere [82, 83].

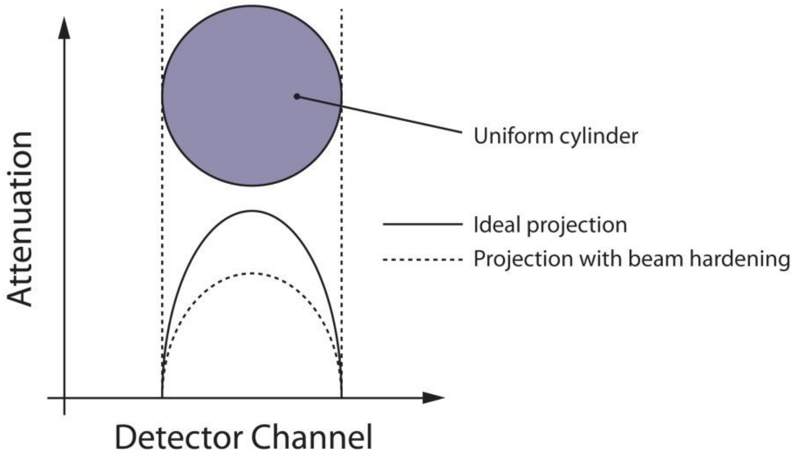

Figure 23. Cupping due to beam hardening

5.4 PARTIAL VOLUME ARTEFACTS

Partial volume artefacts are caused by the limited field of view of the XCT system, where only part of the sample can be measured completely. However, typical XCT reconstruction algorithms assume that the sample can be seen by the XCT system from any rotation angle. When the entire object of interest is not imaged by the detector, shading artefacts can occur [84]. The true linear attenuation coefficients in the measurement volume cannot be calculated properly due to missing information. Partial volume artefacts can be reduced with numerical estimation. However, the improvements are limited. An example of partial volume artefacts and their correction can be seen in figure 24.

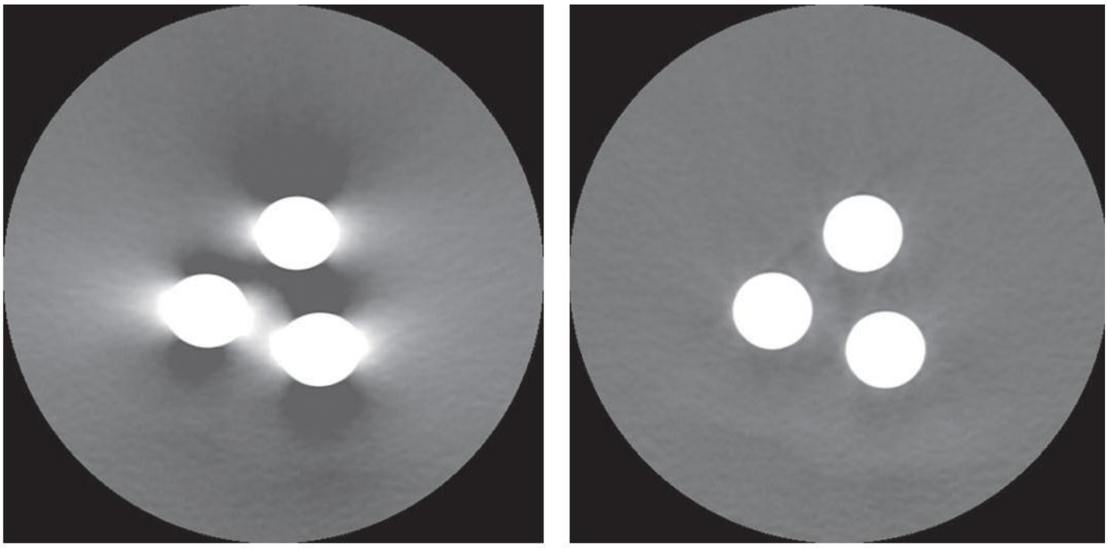

Figure 24. Illustration of partial volume artefacts [67], images of three 12 mm diameter acrylic rods supported in air parallel to and approximately 15 cm from the scanner axis, (left) image obtained with the rods partially intruded into the section width, showing partial volume artefacts, (right) image obtained with the rods fully intruded into the section width, showing no partial volume artefacts

5.5 OTHER SYSTEMATIC ERRORS

The systematic errors mentioned above are unique to XCT systems in comparison with conventional CMMs and hence have been explained in some detail. There are other more generic systematic effects associated with XCT systems, for example the alignment and rotation errors associated with the X-ray source, rotation stage and the detector. As these errors are also common in conventional CMMs, these will not be discussed in this review. More information can be found elsewhere [85, 86].

6 XCT SYSTEM CALIBRATION AND VERIFICATION

Calibration and verification are two processes that are used to evaluate a measurement system. Information on related terminology and definitions can be found in ISO 9000 [87] and VIM [34].

- Calibration

Calibration is the process of comparing the measurement result obtained from the instrument under investigation against that of a known standard, which has an unbroken chain back to national or international standards, with each comparison having a stated uncertainty.

- Verification

Verification is analogous to calibration but returns only a pass/fail result that indicates whether the instrument has been found to be operating within a defined specification, such as published performance data provided by the instrument manufacturer.

6.1 XCT SYSTEM CALIBRATION

When calibrating a system, it is important to know the influence factors that may lead to systematic errors. Examples of influence factors that are known to contribute to errors in dimensional data obtained from a XCT system are listed in table 3. This is not an exhaustive list and, as the subtleties of operation of each XCT system become better understood, more error sources are likely to be added.

Table 3. Examples of error sources in 3D XCT measurements

Type of cause	**Influence factors**
Environment	temperature, humidity, vibration, dust
Object	surface roughness, penetration depth, material composition
Detector	sensitivity, dynamics, quantum efficiency, internal scattering
X-ray source	spectral characteristics, focus properties, opening angle, stability and thermal drift
Manipulation system	geometrical errors, mechanical stability, wobbling
Data processing	reconstruction, threshold determination, filtering, algorithm implementation, artefacts
Other factors	clamping system, object orientation, source current, image statistics

There is increasing interest in XCT calibration in recent years, see for example [14, 15, 88-99]. Due to the importance of the X-ray source and detectors, their calibration is discussed in detail in this section.

Current studies of X-ray sources focus on the characteristics of the focal spot, *i.e.*, the size and shape [92]. Measurement methods for spot size are discussed elsewhere [93-95]. International standard BS EN 12543 part 5 [96] specifies a method for the measurement of focal spot dimensions between 5 µm and 300 µm and the study has been extended to sub-micrometre spot sizes in [97]. However, the effect of X-ray tube current and voltage on focal spot size should be taken into account [100, 101]. Also, the dimensional stability of the focal spot is important as discussed in sections 3.1 and 5.1.

XCT systems operate by determining the difference in intensity between the initial emitted radiation and the absorbed radiation. It is, therefore, critical that these two intensity values are accurately determined. To this end, the detector system needs to be evaluated [102] with and without the presence of radiation. There is commercially available equipment for the calibration of cone beam XCT detectors [103] through the use of calibration standards. Defining the boundary between one material and the other becomes more difficult if the atomic numbers of the two interfacing materials are closely matched - this is due to the variation in what is referred to as the greyscale.

The calibration of a detector is generally carried out by analysing the detector signals with and without incident X-ray illumination. Each pixel in the detector is examined for each case, and its output used to give a calibration response for the radiation dose. Pixels that have no response are assigned the average value of the adjacent pixels in order to compute the associated voxel densities. Noise in the detector has a tendency to decrease the difference in the greyscale between the two materials.

6.2 XCT SYSTEM VERIFICATION

CMMs are generally categorised into two types: contact and non-contact systems. Tactile CMM systems belong to the contact type, and optical systems and XCT systems effectively belong to the non-contact type.

In 2000, the release of ISO 10360 part 1 [104] provided the latest definition of ‘acceptance test’ and ‘reverification test’ for CMMs. ISO 10360 part 1 was further extended with the focus on tactile systems [105-109] and recently added guidance for CMMs with imaging probing systems [110]. Based on the ISO 10360 standards, the verification of CMM systems was detailed in [111]. The definition of CMM verification is given as ‘a task carried out at periodic intervals (often annually) to determine if the CMM still meets the manufacturer’s specification.’

The principle of tactile system verification is detailed in ISO 10360 part 2 and part 5 [105, 108]. The standard recommends comparing the indicated value of five different calibrated and traceable test lengths relative to their calibrated values. The acceptance criterion is that the length error and repeatability, with the consideration of uncertainty, is within the maximum permissible errors specified by the manufacturer. The procedure of imaging probing system verification in ISO 10360 part 7 [110] and contains more detail compared to that related to tactile systems. ISO 10360 part 7 requires the investigation of squareness errors and probing errors.

Currently, there is no international standard that provides comprehensive guidance for system verification for XCT. Although an XCT system is effectively a CMM, its operation is not straightforward compared to conventional tactile and optical systems and the errors associated with the measurements are of a different nature as discussed in section 5.

6.3 INTERNATIONAL STANDARDS FOR XCT TECHNOLOGY

Although there is no published international standard that covers the calibration and verification of XCT systems as discussed in section 6.1 and 6.2, more awareness is being given to the field by a number of international standard committees. There are currently a number of standards related to XCT technology in published or draft form (see table 4).

Table 4 XCT related international standards

Standard	Title
ISO 15708-1 [29]	Non-destructive testing - Radiation methods – Computed tomography – Part1: Principles
ISO 15708-2 [112]	Non-destructive testing – Radiation methods – Computed tomography – Part 2: Examination practices
ISO/TC 213 WG10 [113]	Geometrical product specifications (GPS) – Acceptance and reverification tests for coordinate measuring machines (CMM) – Computed tomography
ASTM E 1695 [114]	Standard test method for measurement of computed tomography (CT) system performance
ASTM E 1441 [115]	Standard guide for computed tomography (CT) imaging
ASTM E 1570 [116]	Standard practice for computed tomographic (CT) examination

International standards [29] and [115] are the most important documents. They provide a clear list of terminology covering most common terms encountered in XCT technologies. Both documents are structured in a similar way, and include the resolution of XCT systems, the apparatus, the general principle of XCT technology, the mathematical background, interpretation of results and a discussion of precision and accuracy. Both documents introduce the important term ‘system capabilities’ (see section 6.4).

International standard ISO 15708 part 2 [112] provides a guideline of procedures for XCT examination practices. A list of data acquisition parameters, image reconstruction parameters and image display parameters are provided in the document, which can be used for developing examination protocols.

International standard ASTM E1695 [114] describes the test method to evaluate the spatial resolution and the contrast sensitivity of an XCT system. The proposed method is to image a uniform disk of material, where the resulting image is immune to cupping artefacts. The operation and analysis procedure is detailed in the standard.

At the time of writing, there is a working document being discussed in ISO/TC 213 WG10 [113] based on German documents VDI/VDE 2630 [117-119]. The working document will be part of the ISO 10360 series, and specifies the acceptance test for verifying the performance of XCT systems with consideration of length errors. However, the document is not currently available to the public.

Generally speaking, the existing international standards mainly cover the terminology and the theory of XCT. Some standards introduce the experimental work regarding determination of spatial resolution, however, there is no comprehensive guideline for system calibration and verification.

6.4 SYSTEM CAPABILITIES

ISO 15708 Part 1 and ASTM E 1441 [29, 115] suggest investigation of the spatial resolution, statistical noise and artefacts when evaluating the capabilities of an XCT system. However, to a broader extend, the evaluation of an XCT system should also consider general dimensional information, for example, what is the largest object that can be measured, what is the smallest feature that can be detected, what is the maximum thickness of sample that the X-ray beam can penetrate, and so on.

6.4.1 Spatial resolution

Spatial resolution is a term defining the ability to image fine structural detail in an object. It is generally quantified in terms of the smallest separation at which two points can be distinguished as separate entities [115]. As with optical systems, the resolution is generally defined in terms of either the Rayleigh or the Sparrow criteria [120-122], which are functions of the wavelength of light used and the numerical aperture of the optical system. In practice, spatial resolution can be characterised by the point spread function (PSF) in the space domain or in terms of the modulation transfer function (MTF) in the frequency domain (see [29, 115, 123] for more information).

An experimental procedure for obtaining the MTF is given in [115], where the MTF can be obtained by following the procedure shown in figure 25. Different experimental methods are also available to determine the MTF [124, 125].

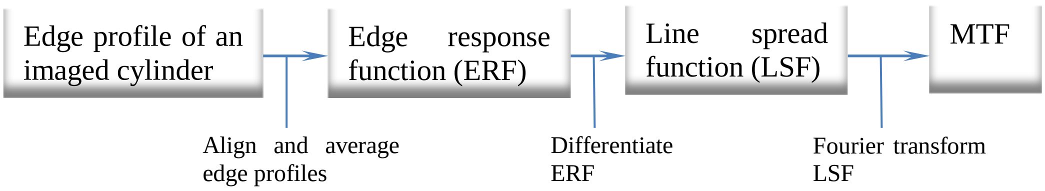

Figure 25. Example test procedure for obtaining the MTF [115]

The report [126] discusses the difference between the MTF and the contrast measurements at line-pair structures [126, 127]. One disadvantage in using the wire (cylinder) is that its profile is only a few pixels in width, and thus the radial PSF is highly under-sampled. Another disadvantage is that the use of the wire does not allow the longitudinal PSF to be calculated [125]. Grimmer *et al* [125] recommend the use of a large sphere (25.4 mm diameter polyoxymethylene sphere) to assess the PSF and the MTF from a single image. This is a divergence from the more prominent method of using a wire, whose diameter is far less than the spatial resolution of the scanner. They also show that through just one image and one reconstruction, both the lateral and the longitudinal PSF can be calculated.

It should be noted that the other term 'detectability' often used is defined differently to spatial resolution. The definition given by ISO 15708 part 1 [29] is the presence of a feature that can be reliably inferred from a tomographic inspection image. It is dependent on system resolution, system noise and size of the feature. A small feature cannot be resolved but may be able to be detected if the contrast is sufficient. A feature can be discriminated only if it can be detected and resolved [29].

6.4.2 Artefacts

Artefact is the term used by the XCT community to denote any systematic discrepancy between the XCT measurement value in the reconstructed image and the true attenuation coefficients of the object (refer to section 5 for more detail). Artefacts can be grouped into subsets such as:

- physics-based artefacts, which result from the physical processes involved in the acquisition of XCT data;
- scanner-based artefacts, which result from imperfections in the motion control system; and
- computer-based artefacts, which are produced by the image reconstruction process.

6.4.3 Statistical noise

Statistical noise arises due to the finite number of photons and the instrumentation and processing used [115]. Noise can be reduced by increasing the scan time, the output of the X-ray source, or the size of the X-ray source and detectors [115, 128]. The impact of statistical noise on different image reconstruction algorithms has been studied elsewhere [128, 129].

6.5 REFERENCE OBJECTS

Reference objects are necessary for system calibration and verification. There are many reference objects of differing dimensions and materials that are currently used to assess different CT systems. They are reviewed in the following sections.

6.5.1 PTB

Scientists at the Physikalisch-Technische Bundesanstalt (PTB), the German national metrology institute, have been investigating uncertainty and traceability of XCT systems for some time, both on their own and in collaboration with other laboratories. PTB is working in a number of relevant areas including uncertainties [130], development of reference objects [131, 132], freeform measurement [133] and general view of XCT technology for dimensional metrology [23].

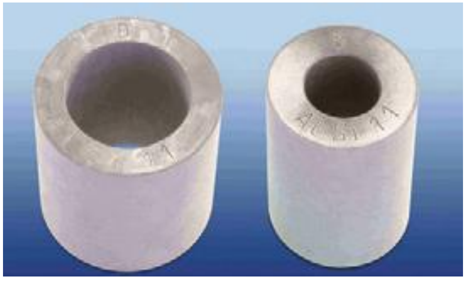

a. Aluminium hollow cylinders (outer diameters 30 mm and 20 mm, respectively)

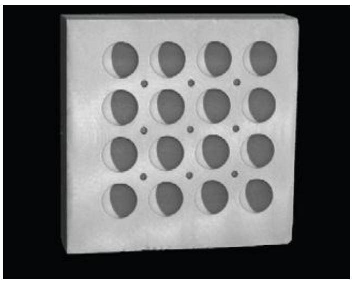

b. Sphere calotte plate made from Zerodur

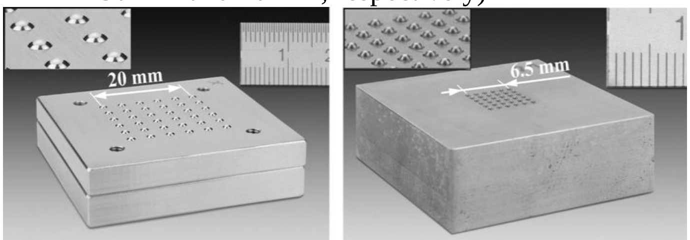

c. Micro-ball plate

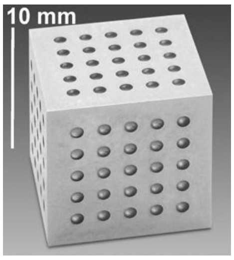

d. Calotte cube

e. Ball-bar (ceramic ball diameter of 30 mm, 100 mm apart, with carbon fibre rod), to assess scale errors

f. Aluminium step-cylinder (outer diameter of 300 mm)

Figure 26. Reference objects developed by PTB [131, 132]

PTB has developed several XCT reference objects [131, 132], which can be seen in figure 26. The procedures for testing tactile and XCT systems are summarised in [131] and the traceability is discussed in [130] (refer to section 6.6 for more information of traceability).

PTB scientists also reported on the use of a cast part of size 120 mm × 90 mm × 60 mm made of aluminium as a reference object [133] (see figure 27). Different to other reference objects developed, this object is dismountable and each segment contains reference objects of standard geometry (ruby spheres of 3 mm diameter) to determine the relative position of each segment.

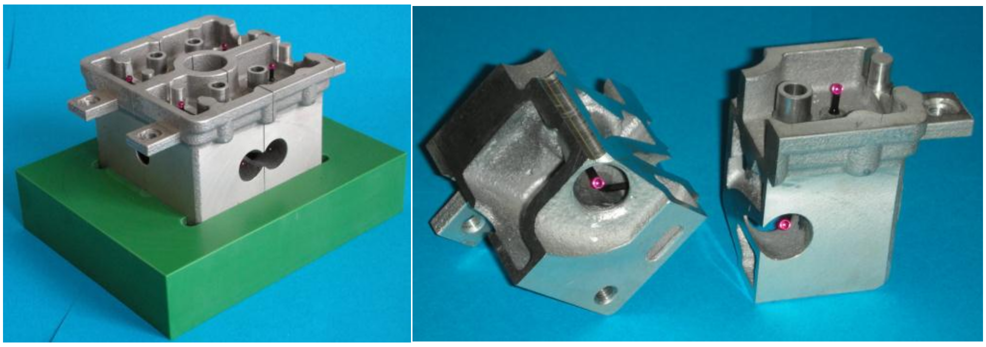

Figure 27. Cast part developed by ACTech GmbH [133] (left) work-piece-near reference object on holding plate (right) two of the four segments of the reference object

6.5.2 Zeiss

Zeiss has also developed dedicated calibration objects and software for the initial configuration and verification of XCT systems. Figure 28 shows one such calibration object, consisting of twenty-seven ruby spheres used to determine the accuracy and repeatability of measurements [134]. The traceability of the form and coordinates of the centre of the spheres is derived from tactile CMM measurements.

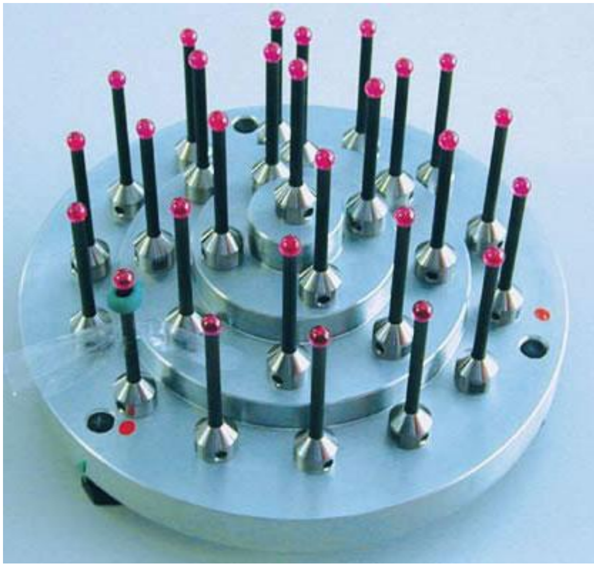

Figure 28. Zeiss calibration reference sphere [134]

Where XCT systems incorporate rotary and translation tables, the performance of the tables needs to be evaluated so that results can be included in the overall performance evaluation of the system. Zeiss have developed several objects for investigating the squareness of their translation stages, as well as the squareness and precession of the rotation axis of their rotary stage with respect to the X-ray source. Included in their software are routines that calculate and correct for the effects of beam hardening. There is also the facility to incorporate different materials, allowing the software to evaluate and store different threshold values.

6.5.3 International comparison of micro-CMM and XCT systems

In 2009 an international comparison of micro-CMMs and micro-XCT was initiated. Participants were VSL (Netherlands), NPL, PTB and METAS (Switzerland), where METAS performed the function of the pilot laboratory. Reported as the first comparison of such systems, this comparison used five comparatively simple objects. These objects are as follows.

1. 85 mm × 85 mm ballplate.
2. 4 mm diameter sapphire sphere.
3. 1 mm diameter silicon nitride sphere.
4. 3 mm diameter by 4.6 mm tungsten carbide ring gauge.
5. Tetrahedral group of four 0.5 mm diameter sapphire spheres.

Of the five objects, two were not measured using XCT; the ballplate due to its size and the ring gauge due to the aspect ratio of the object that led to too much beam hardening. The objects that were measured by XCT systems are shown in figure 29, figure 30 and figure 31. The results from this comparison are yet to be published.

Figure 29. 4 mm diameter sphere

Figure 30. 1 mm diameter sphere

Figure 31. Tetrahedral group of 0.5 mm spheres

6.5.4 CT Audit comparison

The international comparison 'CT audit' [135] is the first international comparison on XCT systems for dimensional metrology. The project is a round robin format comparison organized by the Laboratory of Industrial and Geometrical Metrology at the University of Padova, Italy. The participants in the comparison are institutions, companies and national measurement institutes in Europe, America and Asia [136]. There are four objects that were used in the comparison, as shown in figure 32.

The 'CT Tetrahedron' is a carbon fibre frame with four calibrated ruby spheres. It is provided by the University of Padova. The sample consists of four ruby spheres of size 0.5 mm, attached to the end of a stem. The 'Pan Flute Gauge', also provided by the University of Padova, is a carbon fibre frame with five calibrated glass tubes of different lengths. The 'Calotte Cube' provided by PTB, is a 10 mm × 10 mm × 10 mm titanium cube manufactured using electro-discharge machining. The calottes are 0.8 mm in diameter with a nominal form deviation of less than 2 µm. The 'QFM Cylinder' is a titanium cylinder and a ball plate with five sapphire balls provided by the University Erlangen-Nuremberg. More information can be found on the CT Audit's official website [135].

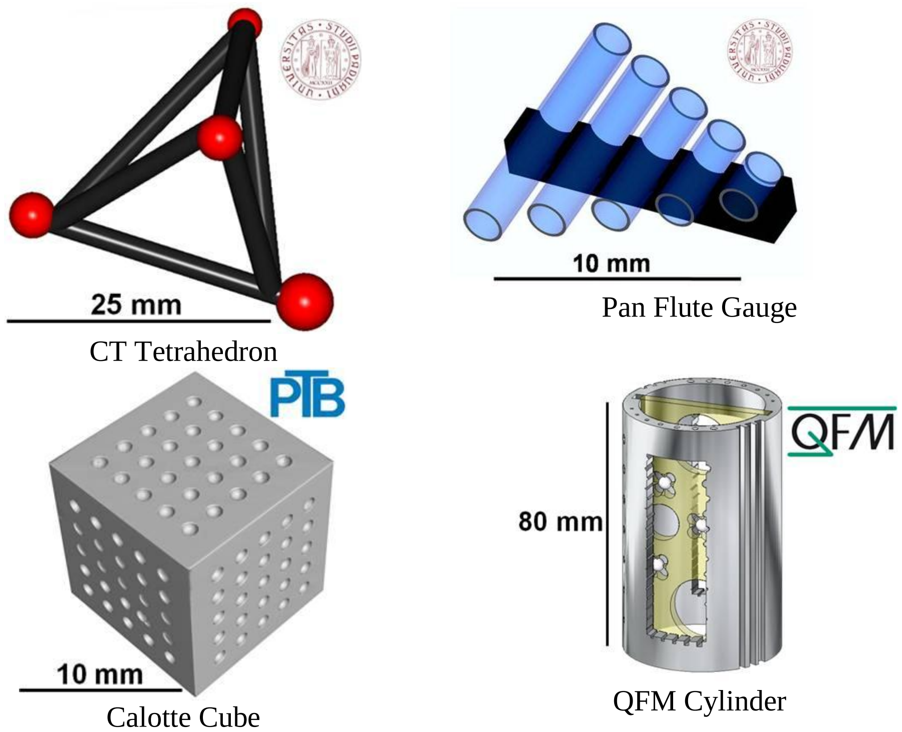

Figure 32. CT Audit items [136]

There are in total fifteen participants, each participant received detailed measurement procedures, reporting sheets, CAD models of the objects and their nominal values. All four items were enclosed in cylindrical boxes manufactured from 0.8 mm polyethylene and the participants were requested not to remove the items from their boxes. The results from the audit are anonymous. The main objective and benefits of the audit, are to deepen the knowledge of XCT dimensional metrology and to spread information on the available reference geometrical standards and procedures for the metrological verification of XCT systems [137].

In total fifteen XCT systems were used to measure the 'CT Tetrahedron'. Measurements were made of the form, diameter and the separation of the spheres. The results from the measurements obtained by the participants, for diameter and sphere separation are closer to the calibrated values than those of the form error, taking into account their stated uncertainties.

The 'Pan flute Gauge' had its inner and outer diameters and the tube lengths measured by fifteen XCT systems. Highlighted in the audit was the fact that a trend was observed, where the inner and outer diameters deviated from their calibrated values in a 'mirror distribution'. The majority of the inner diameters had a negative deviation from reference value and those of the outer diameter exhibited a positive deviation from the reference value. It is mentioned in the audit that this systematic trend will be further investigated. At the end of the audit in March 2011, the calibrated values of the tube diameters were forwarded to the participants, to allow corrections to be made. Six participants returned their corrected values, most showing significant improvement after correcting systematic errors due to thresholding values and scaling.

The 'Calotte cube' was measured by twelve XCT systems. Each participant was asked to report the centre distances, the diameters and the form errors of the calottes. The audit reported that the distance measurements were better than the diameter measurements and the diameter measurements were better than the form error. However, the measurement results showed that all participants overestimated the form error measurements of the calottes.

Measurements on the ‘QFM Cylinder’ were reported for eight XCT systems. This item was found to be the most challenging item to measure, participants were asked to measure: inner and outer diameters of cylinders, calotte diameters, sphere centre distances and diameter of the smallest cylindrical micro structure. Due to the size of the item, not all the participants were able to measure the complete sample. Results from one of the participants were highlighted to show the difference in the measurement deviations of the top calottes diameters using two different procedures [136]. One measurement was to scan the whole item, and the other was to scan only the top calottes with the top calottes in the central plane of the measurement field with a different magnification and thus voxel size. The results show that the second measurements made are generally closer to the calibrated values.

The report concluded that the most accurate measurements were made on the distance between spheres. The higher deviation measurements were on form error, and correct measurement uncertainties were difficult to evaluate due to the numerous influences in XCT measurements.

6.5.5 Other reference objects

Carmignato *et al.* [138] present the first results of a test procedure implemented for determining the errors of indication for the length measurements using XCT systems, using a reference object, referred to as the ‘fibre gauge’, featuring a regular array of inner and outer cylindrical geometries (see figure 33).

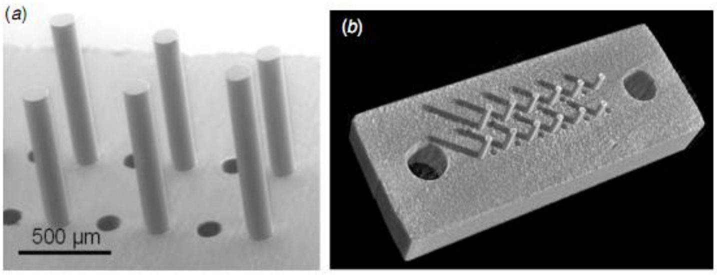

Figure 33. Reference objects developed by Carmignato *et al* [138]

Carmignato *et al.* also describe a solution to the threshold value selection for the item shown in figure 33. The optimal threshold value can be accurately evaluated by, for example, the simultaneous measurement of the calibrated internal and external diameters of the cylinder. The rotational symmetry allows a best-case threshold to be set.

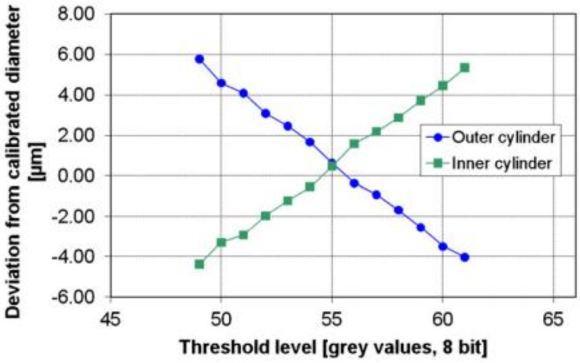

Figure 34. Determining the threshold value [138]

Figure 34 shows the influence on calculated diameter due to the variation in the threshold value. It is important to note that diameters of inner and outer cylinders depend on the changing threshold in the opposite way, increasing the threshold value increases the diameter of the internal cylinders and decreases the diameter of the external cylinders. It is clear that the determination of an incorrect threshold value will give a systematic shift in the calculated position of the object surface or layer interface.

Figure 35 shows a cactus step gauge. It is a 45 mm × 45 mm × 45 mm aluminium block [139], which was used in the investigation of the edge threshold with different influence parameters.

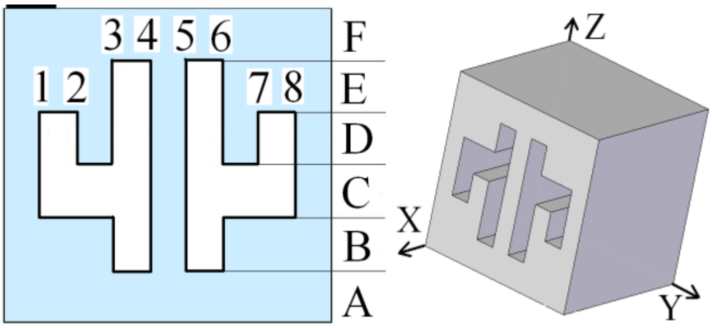

Figure 35. The aluminium cactus block [139] (left) front view (right) 3D model of the sample

Schmitt and Niggermann describe a procedure to evaluate a calibrated workpiece, manufactured from aluminium and measured using tactile CMMs and XCT systems [140] (see figure 36). The effect of several influence parameters (tube voltage, current, filter, exposure time and detector sensitivity) on the uncertainty was analysed.

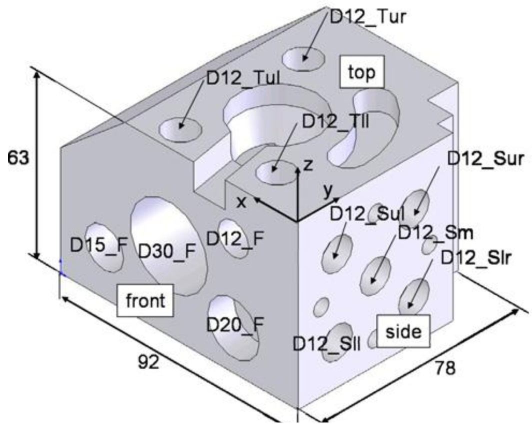

Figure 36. CAD model of workpiece [140]

6.6 DESIGN OF REFERENCE STANDARDS

The growing use of XCT systems to quantitatively measure, as well as to inspect, the internal and external dimensions of simple and complex parts was discussed in section 2.2. As with any dimensional measurement technique, traceability of the measurement instrument to the metre is essential for useful interpretation of generated data.

The *VIM* [34], defines metrological traceability as 'property of a measurement result whereby the results can be related to a reference through a documented unbroken chain of calibrations, each contributing to the measurement uncertainty'. In the case of XCT systems, this traceability, more often than not, is through the calibration of objects by means of tactile CMMs. Furthermore, the document [34] continues to express, that for measurements with more than one input quantity in the measurement model, each of the input quantity values should itself be metrologically traceable and the calibration hierarchy involved may form a branched structure or a network. The effort involved in establishing metrological traceability for each input quantity value should be commensurate with its relative contribution to the measurement result.

From section 6.5, it can be seen that there are many reference objects that are currently being used to give traceability to XCT systems [136]. Some of these objects are being incorporated into the standardization process [119], for example the Calotte Cube developed by PTB and the Micro Tetrahedron developed by the University of Padova [137]. However, a few issues need to be addressed regarding the design of reference standards:

- An ideal situation would be to have an object that allows any XCT system to be calibrated at any setting. However, XCT systems have a multitude of influence parameters, for example, the source energy and the threshold. Unfortunately, changing these parameters has an effect on the response of the system. To design and build a single object that has a predictable response to these different parameters is problematic.

- Another issue that needs to be considered is the beam hardening. This effect is due to the fact that the X-ray photons emitted from the X-ray source have a range of energies (see figure 1). As the X-ray beam passes through the object the lower energy photons are absorbed, which has the resultant effect of increasing the mean energy of the beam and causes artefacts in the reconstructed image (for more information on beam hardening, see section 5.3).

- Objects consisting of multiple materials or composites can be problematic as interfaces between different materials may become blurred or biased towards a particular material in the event that the wrong edge threshold is used. Multiple material objects also cause artefacts and increase noise in the analyses. In an ideal situation, when either calibrating or verifying any XCT system, the atomic number of the calibration object should be the same as the atomic number of the objects under examination, so that an appropriate threshold value can be determined for the interface under examination. An investigation into problems that can occur is given in [23], where materials of steel, rubber and zirconium oxide have been used.

- One of the advantages of XCT systems is the ability to measure, in a non-destructive way, the internal dimensions of an object and surfaces with high aspect ratio. It is this advantage that can become problematic when trying to achieve a traceable calibration chain for features with high aspect ratio, internal dimensions and positions of material interfaces.

Due to the issues discussed above, there is no single calibration object that satisfies all the varying parameters, such as threshold and scale, which influences the metrology of XCT systems. There are manufacturers' claims of the existence of such objects, but in reality they generally only address part of the problem, such as scale.

7 COMMERCIALLY AVAILABE INDUSTRIAL XCT SYSTEMS

The market of XCT manufacturers and their products is briefly reviewed elsewhere [141]. This treatment has been further extended here with more consideration given to industrial XCT systems (see table 5).

Table 5. Manufacturers of industrial XCT systems

Company	Web site, location	Market focuses
Carl Zeiss AG	www.zeiss.com Oberkochen, Germany	Castings Plastics technology Electronics Automation
GE Sensing & Inspection Technologies	www.ge-mcs.com/ Wunstorf, Germany	Material science Plastics engineering Geology/biological sciences Casting & welding Sensorics and electrical engineering
Nikon Metrology NV	www.nikonmetrology.com/ Tring, United Kingdom	Microchip Turbine blade Casting part
Nordson Corporation	www.nordson.com/ Aylesbury, United Kingdom	Printed circuit board assembly Failure analysis Semiconductor
Skyscan	www.skyscan.be/ Kontich, Belgium	Biomedical Material science Electronics Geology
North Star Imaging Inc.	www.xviewct.com/ Minnesota, United States	Aerospace & aviation Medical devices & pharmaceutical Castings Plastics Electronics Museum Dental
Werth Messtechnik GmbH	www.werth.de/ Düsseldorf, Germany	Plastics/hybrid plastics Light/high density metal
Xradia Inc.	www.xradia.com/ California, United States	Material science Geology sciences Semiconductor

In the following sections, detailed information on these industrial cone beam XCT systems is given. Due to limited resources of information, this market review is based on information publicly available at the time of writing. Hence it may not cover all the latest product developments. Readers should always seek information from manufacturers directly. Also, it has to be noted that some terms used in system specification in the sections 7.1 to 7.8 are non-standard terms. For example, detectability is a non-standard term that has been used by some manufacturers, to indicate the performance of their system.

The main interests of the following sections are focused on the capability of the X-ray tube and the detector, as they determine the main application of the particular products. Other specifications, such as dimension of measurement chamber, environmental stability and number of available axes are not discussed here. As different manufacturers provide different information, there is no cross-comparison of these products. Options for user-specified machines are also excluded from consideration. Only information available from these companies' websites has been used in the following section.

7.1 CARL ZEISS AG

Carl Zeiss AG, headquartered in Oberkochen, Germany supplies a broad range of imaging and metrology products for various industries. In terms of its XCT systems, the Metrotom CT system has been available since 2004, and the systems were developed for dimensional metrology purposes. The data can be analysed using Carl Zeiss' generic CAD-based metrology software package Calypso, in which the user can compare XCT measurements of an object with the CAD model of the object. A summary of systems is presented in table 6. Information that is not available is indicated as 'n/a' in the table.

Table 6. Summary of Carl Zeiss XCT systems

Model	Maximum voltage /kV	Power /W	X-ray spot size /µm	Detector	Maximum object size (diameter × height) /(mm × mm)
Metrotom 800	130	39	n/a	n/a	125 × 150
Metrotom 1500	225	225	n/a	n/a	350 × 350

7.2 GE SENSING & INSPECTION TECHNOLGIES

GE Sensing & Inspection Technologies (GE) is a company based in United States. In 2007 GE acquired Phoenix|x-ray, whose production research and development activities are located in Wunstorf, Germany. GE's current XCT products range in power from 15 W to 1500 W. GE has also developed their own X-ray tube and X-ray detector. The 'T nanofocus' X-ray tubes have a detail detectability of 0.2 µm and the 'D microfocus' X-ray tubes have detectability up to 1 µm. The DXR series X-ray detector developed by GE covers a wide range of applications, from radiography to XCT. The DXR 250 RT real-time digital detector array has an active area of 205 mm × 205 mm and a frame rate of 30 frames per second. The flat panel consists of an amorphous silicon detector with a CsI scintillator. The details of these systems can be found in table 7.

Table 7. Summary of GE XCT systems

Model	Maximum voltage /kV	Power /W	X-ray detectability /µm	Common detector	Maximum object size (diameter × height) /(mm × mm)
nanotom m	180	15	0.2		240 × 250
nanotom s	180	15	0.2		120 × 150
v|tome|x s	240	320	1		135 × 420
v|tome|x L 240	240	320	1	GE DXR detector	500 × 600
v|tome|x L 300	300	500	1		500 × 600
v|tome|x L 450	450	1500	1		800 × 1000

Apart from the development of hardware, GE has also developed their phoenix datos|x 2.0 – CT software. The software provides data reconstruction, volume optimization (for example, beam hardening correction) and surface extraction. The software also has functions that allow the user to analyse the data.

7.3 NIKON METROLOGY NV

Nikon XCT systems were formerly branded as X-tek, which was acquired by Metris in 2007; Metris was then acquired by Nikon in 2009. Currently, Nikon supply four main models, ranging in maximum voltage from 160 kV to 450 kV. The detail can be seen in table 8. These systems use open tube ultra-focus reflection targets and have an option of using a transmission-type target. The detectors used are generally provided by Varian or Perkin Elmer. All of these detectors use amorphous silicon.

Table 8. Summary of Nikon XCT systems

Model	Maximum voltage /kV	Power /W	X-ray spot size /µm	Detector area /(mm × mm)	Maximum inspection area /(mm × mm)
XT H 160	160	225	3	130 × 130	n/a
XT H 225	225	225	3	195 × 244	250 × 330
XT H 320 LC	320	320	20	195 × 244	n/a
XT H 450 3D	450	450	80	400 × 400	n/a

7.4 NORDSON CORPORATION

Table 9. Summary of Nordson Dage XCT systems

Model	Maximum voltage /kV	Power /W	Feature recognition /µm	Detector	Maximum inspection area /(mm × mm)
XD7600NT Ruby	160	4	0.5	χiDAT3 (2 megapixels)	508 × 444
XD7600NT Ruby FP	160	4	0.5	CMOS digital detector (1.3 megapixels)	508 × 444
XD7600NT Diamond	160	4	0.1	χiDAT3 (2 megapixels)	508 × 444
XD7600NT Diamond FP	160	4	0.1	CMOS digital detector (3 megapixels)	508 × 444
XD7800NT 100HP	160	4	0.1	χiDAT (2 megapixels)	610 × 762
XD7800NT950	160	3	0.95	χiDAT (1.3 megapixels)	610 × 762
XD7800NT950 HP	160	10	0.95	χiDAT (1.3 megapixels)	610 × 762
XD7800VR	160	3	0.95	χiDAT (1.3 megapixels)	610 × 762

Nordson Corporation was founded in 1954 with the headquarters in Ohio, United States. The company acquired Dage Holdings Ltd in 2006 and the resultant operation Nordson DAGE is headquartered in Aylesbury, UK. The XCT systems produced by Nordson DAGE use the DAGE NT 100 sealed-transmissive, filament-free X-ray tubes. The value of feature recognition listed in table 9 is for a tube with power below 4 W (with the exception of the XD7800NT950HP system). The XD7600NT series systems use a 16-bit FPD with a maximum inspection area of 508 mm × 444 mm. The XD7800NT series was designed for inspection of semiconductors and large printed circuit boards. The systems use a large FPD with a maximum inspection area of 610 mm × 762 mm. The XD7800NT 100HP system has a frame rate of thirty frames per second. All other systems have a frame rate of twenty-five frames per second.

7.5 SKYSCAN

SkyScan is a Belgium company that focuses on micro- and nano-XCT products. The company was founded in 1996, with the first commercial product released a year later. Products developed by SkyScan generally are smaller than many commercial XCT systems on the market. For example, the size of the SkyScan 1172 system is only 1250 mm (length) × 659 mm (width) × 360 mm (height). The mass of SkyScan systems is generally below 500 kg. The detail can be seen in table 10.

SkyScan has also developed its own XCT software, including NRecon, Data Viewer and Ctvox. NRecon is the reconstruction software, Data Viewer can convert data into different image formats and Ctvox is the visualisation software, which supports functions such as clipping. SkyScan also provides the package CT-analyser for data analysis and CT-volume for advanced data visualisation.

Table 10. Summary of Skyscan XCT systems

Model	**Voltage /kV**	**Power /W**	**Detail detectability /µm**	**Detector**	**Maximum object size (diameter × height) /(mm × mm)**
1172	20-100	10	0.5	11 megapixels, 12-bit CCD fibre-optically coupled to scintillator	50 × 70
1174	20-50	40	6	1.3 megapixels, 14-bit cooled CCD with 1:6 zoom lens	30 × 50
1176	20-90	25	9	11 megapixels, 12-bit CCD fibre-optically coupled to scintillator	68 × 200
1178	20-65	40	80	1.3 megapixels, 12-bit cameras	80 × 200
2011	20-80	n/a	0.2	1.3 megapixels, 12-bit X-ray CCD camera	11 × n/a

7.6 NORTH STAR IMAGING INC.

North Star Imaging Inc. was founded in 1986 and is headquartered in Minnesota, United States. The company provides both open and sealed X-ray tubes. The company also developed software to address data acquisition, processing and archival. Details of their systems can be found in table 11. It is also stated on the company's website that they provide calibrated XCT systems for dimensional metrology.

Table 11. Summary of North Star Imaging XCT systems

Model	Voltage /kV	Power /W	Focal Spot Size /µm	Detector size /(mm × mm)	Maximum sample size /mm
ImagiX	150	n/a	5	250 × 250	150
X50-CT	Sealed Tube: 100, 130, 150	n/a	1	Flat panel/ Linear array, panel size from 100 × 100 to 400 × 400	300
X500-CT		n/a	1		600
X5000-CT	Open Tube: 160, 225	n/a	1		n/a.
EXPRESS-CT	320, 450	n/a	1		n/a

The term 'Maximum sample size' used in table 11 refers to the vertical and lateral axes travel relative to the scanning envelope.

7.7 WERTH MESSTECHINK GMBH

Werth Messtechnik GmbH was founded in 1951 in Düsseldorf, Germany. In contrast with other XCT developers, Werth Messtechnik is focused on developing multi-sensor systems. The first multi-sensor coordinate measuring machines with XCT was developed in 2005. More information about their XCT systems is available in table 12. For each model, the company allows users to choose from a range of setups.

Table 12. Summary of Werth Messtechnik XCT systems

Model	Maximum voltage /kV	Power /W	Resolution /µm	Detector size /(mm × mm)	Maximum object size (diameter × height) /(mm × mm)
TomoScope 200	130 150 190	n/a	0.1	50 × 50 130 × 130	110 × 200
TomoCheck 200	130 150	n/a	0.1	50 × 50	90 × 200
TomoScope HV Compact	225	n/a	0.1	n/a	330 × 350
TomoScope HV 500	225	n/a	0.1	400 × 400	350 × 500

7.8 XRADIA

Xradia was founded in 2000 and is based in California, United States. The company designs, develops and manufactures micro- and nano-XCT systems. Apart from the systems listed in table 13, the company also provides synchrotron X-ray microscope systems with 30 nm resolution. However, it is unclear how the resolution has been determined. The company also integrated a Zernike phase contrast plate to enhance the visibility of edges and interfaces when contrast is low. The VersaXRM-500 system also allows users to do *in situ* measurements and time-dependent studies.

Table 13. Summary of Xradia XCT systems

Model	Maximum voltage /kV	Power /W	Spatial resolution /μm	Detector size /(mm × mm)	Sample size /mm
MicroXCT-200	20-90	8	1	n/a	150
MicroXCT-400	40-150	10	1	n/a	300
					Field of view /μm
VersaXRM-500	30-160	10	0.7	n/a	n/a
UltraXRM-L200	20-40	1200	0.05	n/a	15 to 60

7.9 UK INSTITUTIONS AND XCT RELATED WORK

XCT technology, especially with regards to industrial application, is a relatively new research field. The recent increase in numbers of XCT systems owned by universities indicates an increase in XCT research activities. Table 14 lists a few institutes that currently host XCT systems. NPL is currently collaborating with the University of Southampton and the University of Manchester. Both universities have strong research teams working on XCT and related aspects. There are also other UK universities that own XCT facilities, such as University of Leicester, University of Leeds and University of Nottingham, responding to a demand for XCT in various research fields.

Table 14. Summary of UK universities that with XCT systems

Name of Institution	XCT facilities
University of Southampton (μ-VIS)	Nikon custom 225 kV/450 kV hutch Nikon custom 225 kV Nikon 160 kV benchtop Gatan XuM/Zeiss Evo MA25 SkyScan 1176 in vivo CT
University of Manchester (Henry Moseley X-ray Imaging Facility)	Nikon/Metris custom 320 kV bay Nikon/Metris XTH225 kV Xradia MicroXCT Xradia nanoXCT Rapiscan RTT20
University of Leicester	Nikon/Metris 225 kV
University of Leeds	GE/Phoenix Nanotom
University of Loughborough	Nikon/Metris XT H
University of Nottingham	GE/Phoenix Nanotom
University of Warwick	Nikon/Metris 320 kV
University of Huddersfield	Nikon XTH 225 kV

8 CONCLUSIONS

In this report, the market trend of industrial XCT systems has been reviewed and recent developments of both XCT hardware and software studied. Latest products on the market have also been reviewed; the unique systematic errors associated with XCT systems discussed and recent developments regarding the calibration and verification of XCT systems reviewed. It is clear that the industrial XCT market is growing rapidly and there is a significant demand to use the technology to detect faulty parts and to provide dimensional information about measured samples. However, the development of the technology is still in its infancy.

Based on this report, there are a number of issues that need to be addressed. Using XCT as a dimensional tool, requires the determination of the surface boundary, which is based on the measured volumetric data. These boundaries can be significantly affected by the selection of the threshold value, which relies heavily on the empirical knowledge of the operator. This report has shown that there is no universal technique for predicting the correct threshold value. It is also unclear for manufacturers, as well as end users, how to evaluate systems, as there is no complete system verification procedure available that can be followed. Furthermore, there are terminology issues found in the manufacturers' literature, where terms, such as 'feature recognition', 'maximum inspection area' and 'maximum object size', have no definition and are, therefore, causing confusion.

In the future, a user guide defining terminology, from both the CMM and XCT environment would be a useful starting point. This should be followed by the development of verification objects and surface determination methods. In parallel to this, a system verification procedure should be developed, incorporating methods for XCT calibration based on a study of systematic errors. All this work is required urgently to develop a traceability infrastructure for measurements using XCT systems.

ACKNOWLEDGEMENT

This report and the underlying NPL XCT project were funded by the National Measurement Office (NMO) Engineering Measurement and Flow Programme. The project is additionally supported by the EPSRC Knowledge Transfer Secondments scheme, via the University of Southampton. Many thanks are due to Professor John McBride and Professor Ian Sinclair for providing access to μ-VIS XCT facilities at the University of Southampton, as well as insight and knowledge in XCT. We would also like to thank Dr Michael McCarthy at NPL, the staff, especially Dr Dmitry Grinev and Dr Mark Noel Mavrogordato at the University of Southampton, Dr Fabien Leonard, Professor Phil Withers and Professor Paul Mummery at the University of Manchester's Henry Molesey X-ray Imaging Facility. Finally, we are grateful to Mr Christopher Jones, Mr David Flack, Dr Andrew Yacoot and Dr Andrew Lewis, for assistance with proofreading.

REFERENCES

[1] Cormack A M and Hounsfield G N 1979 The Nobel Prize in Physiology or Medicine

[2] Thomas S J 1999 Relative electron density calibration of CT scanners for radiotherapy treatment planning *Brit. J. Radiol.* **72** 781-86

[3] Berrington de González A, Mahesh M, Kim K-P, Bhargavan M, Lewis R, Mettler F and Land C 2009 Projected cancer risks from computed tomographic scans performed in the United States in 2007 *Arch. Intern. Med.* **169** 2071-77

[4] Ionising radiation Website: www.npl.co.uk/educate-explore/posters/ionising-radiation/ Accessed on 1st November 2011

[5] Feldkamp L A, Davis L C and Kress J W 1984 Practical cone-beam algorithm *JOSA A: Optics, Image Science, and Vision* **1** 612-19

[6] Weckenmann A, Kraemer P and Hoffmann J 2007 *Manufacturing metrology - state of the art and prospects Proc. of 9th International Symposium on Measurement and Quality Control* (IIT Madras) pp7

[7] January 2011 *Computed tomography (CT) scanners: A global strategic business report* Global Industry Analysts Inc Report MCP-3321

[8] 24th March 2011 Higher standards of quality open up opportunities for X-ray inspections systems (Frost and Sullivan)

[9] Jose S Global installed base of computed tomography (CT) scanners to reach about 60 thousand units by 2015, according to new report by global industry analysts, Inc. Website: www.prweb.com/releases/computed_tomography/CT_scanners/prweb8075828.htm Accessed on 3rd August 2011

[10] Rapiscan Systems Website: www.rapiscansystems.com/ Accessed on 3rd August 2011

[11] Pollitt M 20th March 2008 How X-rays can detect cocaine or semtex in a large suitcase The Guardian www.guardian.co.uk/technology/2008/mar/20/engineering.research

[12] (Security Media Publishing Ltd.) Website: www.securitymiddleeast.com/news/read/american-science-and-engineering-inc-receives-82-million-order-for-its-cargo-inspection-systems-to-secure-critical-infrastructure-in-the-middle-east-2010-04-01 Accessed on 29 September 2011

[13] Flack D and Hannaford J 2005 *Fundamental good practice in dimensional metrology* National Physical Laboratory Measurement Good Practice Guide No. 80

[14] Yang K, Kwan A L C, Miller D F and Boone J M 2006 A geometric calibration method for cone beam CT systems *Med. Phys.* **33** 1695-706

[15] Sun Y, Hou Y, Zhao F and Hu J 2005 A calibration method for misaligned scanner geometry in cone-beam computed tomography *Nondestructive Testing* **10**

[16] Holt K M 2007 *Geometric calibration of third-generation computed tomography scanners from scans of unknown objects using complementary rays Proc. of IEEE International Conference on Image Processing (ICIP)* (San Antonio)

[17] Röntgen W C 1896 On a new kind of rays *Sci.* **3** 227-31

[18] Thomson J J 2005 *Conduction of electricity through gases* (Wexford College Press)

[19] Young H D, Freedman R A, Sandin T R and Ford A L 1999 *Sears and Zemansky's university physics (10th Edition)* (Addison-Wesley)

[20] 2007 Industrial radiography image forming techniques (General Electric Company) GEIT 30158EN

[21] Maur F W 2007 *Lastest developments in X-ray microscopy Proc. of International Workshop on Imaging NDE* (Kalpakkam, India)

[22] X-ray tube basics Website: h2g2.com/dna/h2g2/A14017943 Accessed on 1st October 2011

[23] Kruth J P, Bartscher M, Carmignato S, Schmitt R, De Chifffre L and Weckenmann A 2011 Computed tomography for dimensional metrology *Ann. CIRP* **60** 821-42

[24] Daneke N and Schanklies B October 2004 From microfocus to nanofocus X-ray inspection *OnBoard Technology* 42-44

[25] Uhlman N, Salamon M, Burtzlaff S, Porsch F, Johansson W, Nachtrab F and Hanke R 2008 *Components and methods for highest resolution computed tomography Proc. of International Symposium on NDT in Aerospace* (Fürth, Germany) pp7
[26] 1980 Radiography in modern industry (Eastman Kodak Company) Quinn R A and Sigl C C 4th Edition
[27] Rapp-Bernhardt U, Roehl F W, Gibbs R C, Schmidl H, Krause U W and Bernhardt T M 2003 Flat-panel X-ray detector based on amorphous silicon versus asymmetric screen-film system: Phantom study of dose reduction and depiction of simulated findings *Radiology* **227** 484-92
[28] Ewert U 2002 New trends in industrial radiology *NDT* **7**
[29] ISO 15708-1:2002(E) Non-destructive testing – Radiation methods – Computed tomography - Part 1: Principles, International Organization for Standardization
[30] Thompson A, Lindau I, Attwood D, Liu Y, Pianetta E G, Howells M, Robinson A, Kim K-J, Scofield J, Kirz J, Underwood J, Kortright J, Williams G and Winick H 2009 *X-ray data booklet* Lawrence Berkeley National Laboratory, University of California, Berkeley LBNL/PUB-490 Rev. 3
[31] FT50M 1 MP 100fps CCD - product detail - Teledyne DALSA Website: www.teledynedalsa.com/ls/products/sensordetails.aspx?partNumber=FT50M Accessed on 1st December 2011
[32] Cvijetic M 2004 *Optical transmission systems engineering* (Artech House) p303
[33] Yaffe M J and Rowlands J A 1997 X-ray detectors for digital radiography *Phys. Med. Biol.* 1-39
[34] JCGM 200:2008 International vocabulary of metrology - basic and general concepts and associated terms, International Organization for Standardization
[35] Yan H and Mou X 2010 *Projection correlation based noise reduction in volume CT Proc. of Nuclear Science Symposium Conference Record* pp2948-53
[36] Yang K, Kwan A L, Huang S Y, Packard N J and Boone J M 2008 Noise power properties of a cone-beam CT system for breast cancer detection *Med. Phys.* **35** 5317-27
[37] Radiation protection in diagnostic and interventional radiology. Part 12.1: Shielding and X-ray room design practical exercise (International atomic Energy Agency, Austria) Website: https://rpop.iaea.org/RPOP/RPoP/Content/Documents/TrainingRadiology/Practicals/RPDIR-P12.1_Shielding_calculation_WEB.ppt Accessed on 3rd August 2011
[38] Sprawls P The web-based edition of the physical principles of medical imaging Website: www.sprawls.org/ppmi2/XRAYHEAT/ Accessed on 4th August 2011
[39] Schardt P, Deuringer J, Freudenberger J, Hell E, Knüpfer W, Mattern D and Schild M 2004 New X-ray tube performance in computed tomography by introducing the rotating envelope tube technology *Med. Phys.* **31** 2699-706
[40] Brunke O, Neuser E and Suppes A 2011 *High resolution industrial CT systems: advances and comparison with synchrotron-based CT Proc. of International Symposium on Digital Industrial Radiology and Computed Tomography* (Berlin) pp9
[41] New cooling system for microfocus X-ray tubes (X-RAY WorX GmbH) Website: www.x-ray-worx.com/joomla/index.php?option=com_content&view=article&id=126%3Ax-ray-worx-kuehlung-fuer-mikrofokus-roehren&catid=75%3Apressemeldungen-x-ray-worx&Itemid=55&lang=fr Accessed on 4th August 2011
[42] Helgason S 1999 *The radon transform* (Birkhauser Boston) p190
[43] Ketcham R A and Carlson W D 2001 Acquisition, optimization and interpretation of X-ray computed tomographic imagery: applications to the geosciences *Comput. Geosci.* **27** 381-400
[44] Ramachandran G N and Lakshminarayanan A V 1970 *Three-dimensional reconstruction from radiographs and electron micrographs: application of convolutions instead of fourier transforms Proc. of National Academy of Science* (USA) Vol68 pp2236-40

[45] Shepp L A and Logan B F 1974 Reconstructing interior head tissue from X-ray transmissions *IEEE Trans. Nucl. Sci.* **21** 228-36
[46] Kalender W A 2000 *Computed tomography: Fundamentals, system technology, image quality, applications* (Wiley-VCH) p220
[47] Zeng G L and Gullberg G T 1994 *Can the backprojection filtering algorithm be as accurate as the filtered backprojection algorithm? Proc. of Nuclear Science Symposium and Medical Imaging Conference* Vol3 pp1232-36
[48] Smith B D 1990 Cone-beam tomography: recent advances and a tutorial review *Opt. Eng.* **29** 524-34
[49] Turbell H 2001 Cone-beam reconstruction using filtered backprojection Department of Electrical Engineering (Linköpings University) p177
[50] Noo F, Clack R and Defrise M 1997 Cone-beam reconstruction from general discrete vertex sets using radon rebinning algorithms *IEEE Trans. Nucl. Sci.* **44** 1309-16
[51] Imiya J and Ogawa H 1984 *A direct method of image reconstruction from its line integrals by cone-beam x-rays Proc. of International Joint Alpine Symposium on Medical Computing, Graphics Image Communication and Clinical Advances in Neuro CT/NMR, IEEE* (Innsbruck, Austria)
[52] Wang G, Lin T-H, Cheng P-C and Shinozaki D M 1993 A general cone-beam reconstruction algorithm *IEEE Trans. Med. Imaging* **12** 486-96
[53] Finch D V 1985 Cone beam reconstruction with sources on a curve *SIAM J. Appl. Math.* **45** 665-73
[54] Hamaker C, Smith K T, Solomon D C and Wagner S L 1980 The divergent beam x-ray transform *J. Math.* **10** 253-84
[55] Herman G T 2009 *Fundamentals of computerized tomography: Image reconstruction from projections* Singh S (Springer)
[56] Kowalski G 1979 Multislice reconstruction from twin cone-beam scanning *IEEE Trans. Nucl. Sci.* **26** 2895-903
[57] Kowalski G 1977 Fast 3-D scanning systems using a limited tilting angle *Appl. Opt.* **16** 1686-90
[58] Minerbo G N 1979 Convolutional reconstruction from cone-beam projection data *IEEE Trans. Nucl. Sci.* **26** 2682-84
[59] Peyrin F C 1985 The generalized back projection theorem for cone beam reconstruction *IEEE Trans. Nucl. Sci.* **32** 1512-19
[60] Schlindwein M 1978 Iterative three-dimensional reconstruction from twin-cone beam projections *IEEE Trans. Nucl. Sci.* **25** 1135-43
[61] Smith K T 1982 *Reconstruction formulas in computed tomography Proc. of Symposium on Applied Mathematics* Vol27
[62] Tuy N K 1983 An inversion formula for cone-beam reconstruction *SIAM J. Appl. Math.* **43** 546-52
[63] Yang D 2007 Flat panel detector-based cone beam CT: reconstruction implementation and applications for dynamic imaging Department of Electrical and Computer Engineering (University of Rochester) p132
[64] Nikon metrology incorporates inspect-X and CT-pro into XT software suite V2.2 Website: www.nikonmetrology.com/news/recent_news/nikon_metrology_incorporates_inspectx_and_ctpro_into_xt_software_suite_v2.2/ Accessed on 1st October 2011
[65] phoenix datos|x CT software Website: www.ge-mcs.com/en/radiography-x-ray/ct-computed-tomography/datosx-ct-software.html Accessed on 1st October 2011
[66] Lacroute P and Levoy M 1994 *Fast volume rendering using a shear-warp factorization of the viewing transformation, Proc. of Siggraph* (Orlando, Florida) pp451-58
[67] Barrett J F and Keat N 2004 Artifacts in CT: recognition and aviodance *Radio Graphics* **24** 1679-91
[68] Steffen J P and Froba T 2011 *Reducing the focal spot shift of microfocus X-ray tubes to increase the accuracy of CT-based dimensional measurement Proc. of International*

Symposium on Digital Industrial Radiology and Computed Tomography (Berlin, Germany)

[69] Vogeler F, Verheecke W, Voet A, Kruth J-P and Dewulf W 2011 *Positional stability of 2D X-ray images for computed tomography Proc. of International Symposium on Digital Industrial Radiology and Computed Tomography* (Berlin, Germany)

[70] Sijbers J and Postnov A 2004 Reduction of ring artefacts in high resolution micro-CT reconstructions *Phys. Med. Biol.* **49** 247-53

[71] Bock R, Hoppe S, Scherl H and Hornegger J 2007 *Beam hardening correction with an iterative scheme using an exact backward projector and a polychromatic forward projector Proc. of Bildverarbeitung für die Medizin* (Munich, Germany: Springer) pp46-50

[72] Ramakrishna K, Muralidhar K and Munshi P 2006 Beam-hardening in simulated X-ray tomography *NDT & E Int.* **39** 449-57

[73] Van Gompel G, Van Slambrouck K, Defrise M, Batenburg K J, de Mey J, Sijbers J and Nuyts J 2011 Iterative correction of beam hardening artifacts in CT *Med. Phys.* **38** S36-49

[74] Herman G T 1979 Demonstration of beam hardening correction in computed-tomography of the head *J. Comput. Assisted Tomogr.* **3** 373-78

[75] Krumm M, Kasperl S and Franz M 2010 *Beam hardening correction of multi-material objects Proc. of 10th European Conference on Non-Destructive Testing* (Moskau) pp7

[76] Pettersson H, Allison D, von Schulthess G K and Smith H-J 1998 *The encyclopaedia of medical imaging - Volume I: Physics, techniques and procedures*

[77] Alvarez R E and Macovski A 1976 Energy-selective reconstruction in X-ray computerized tomography *Phys. Med. Biol.* **21** 733-44

[78] Seibert J A and Boone J M 2005 X-ray imaging physics for nuclear medicine technologists. Part 2: X-ray interactions and image formation *J. Nucl. Med. Technol.* **33** 3-18

[79] Smith C R, Holt K, Bischoff U, Georgi B, Hansen F and Jeltsch F 2007 Application of 450 kV computed tomography to engine blocks with steel liners *Mater. Eval.* **65** 458-61

[80] Popilock R, Sandrasagaren K, Harris L and Kaser K A 2008 CT artifact recongnition for the nuclear technologist *J. Nucl. Med. Technol.* **36** 279-81

[81] Van de Casteele E, Van Dyck D, Sijbers J and Raman E 2004 A model-based correction method for beam hardening artefacts in X-ray microtomography *J. X-ray Sci. Technol.* **12** 53-57

[82] Kachelriess M, Sourbelle K and Kalender W 2006 Empirical cupping correction: A first-order raw data precorrection for cone-beam computed tomography *Med. Phys.* **33** 1269-74

[83] Zhang L, Gao H, Li S, Chen Z and Xing Y 2006 *Cupping artifacts analysis and correction for a FPD-based cone-beam CT Proc. of SPIE* (San Jose, CA, USA) Vol6065

[84] Lee R D Common image artifacts in cone beam CT Website: www.aadmrt.com/currents/lee_summer_08_print.htm Accessed on 1st October 2011

[85] Balter S, Bassano D, McCullough E C, Payne J T and Rothenberg L 1977 *Phantoms for performance evaluation and quality assurance of CT scanners* American Association of Physicists in Medicine Report No 1

[86] Leach R K 2010 *Fundamental principles of engineering nanometrology* (Elsevier)

[87] ISO 9000:2005 Quality management systems — Fundamentals and vocabulary, International Organization for Standardization

[88] Wein W, Ladikos A and Baumgartner A 2011 *Self-calibration of geometric and radiometric parameters for cone-beam computed tomography Proc. of 11th International Meeting on Fully Three-Dimensional Image Reconstruction in Radiology and Nuclear Medicine* (Munchen, Germany) pp4

[89] Kyriakou Y, Prell D, Kalender W A and Kachelrieß M 2010 Empirical beam hardening correction for CT *Med. Phys.* **37** 5179-87
[90] Grimmer R, Maaß C and Kachelrieß M 2009 *A new method for cupping and scatter precorrection for flat detector CT Proc. of Nuclear Science Symposium and Medical Imaging Conference, IEEE* (Orlando, Florida, USA) pp3517-22
[91] Zhu S, Tian J, Yan G, Qin C and Liu J 2009 Cone beam micro-CT system for small animal imaging and performance evaluation *Int. J. Biomed. Imaging* **2009** 9
[92] Romanov A Y 2004 Measurement of the parameters of the focal spot of an X-ray tube using Kumakhov optics *Meas. Tech.* **47** 670-74
[93] Robinson A and Grimshaw G M 1975 Measurement of the focal spot size of diagnostic X-ray tubes—a comparison of pinhole and resolution methods *Br. J. Radiol.* **48** 572-80
[94] Chen Q, Chen Y, Chen M, Chao E, Sterpin E and Lu W 2011 A slit method to determine the focal spot size and shape of TomoTherapy system *Med. Phys.* **38** 2841-49
[95] Russo P and Mettivier G 2011 Method for measuring the focal spot size of an x-ray tube using a coded aperture mask and a digital detector *Med. Phys.* **38**
[96] BS EN 12543-5:1999 Non-destructive testing. Characteristics of focal spots in industrial X-ray systems for use in non-destructive testing. Measurement of the effective focal spot size of mini and micro focus X-ray tubes, British Standards Institution
[97] Salamon M, Hanke R, Krüger P, Sukowski F, Uhlmann N and Voland V 2008 Comparison of different methods for determining the size of a focal spot of microfocus X-ray tubes *Nucl. Instrum. Meth. A* **591** 54-58
[98] Cho Y, Siewerdsen J H and Jaffray D A 2005 Accurate technique for complete geometric calibration of cone-beam computed tomography systems *Med, Phys.* **32** 968-83
[99] Panetta D, Belcari N, Guerra A D and Moehrs S 2008 An optimization-based method for geometrical calibration in cone-beam CT without dedicated phantoms *Phys. Med. Biol.* **53** 3841-61
[100] Chaney E L and Hendee W R 1974 Effects of X-ray tube current and voltage on effective focalspot size *Med. Phys.* **1** 141-47
[101] Gunnarsson M 1995 Evaluation of a new method for focal spot size measurements - A study on mammography X-ray tubes Radiation Physics Department, University of Gothenburg (Master Thesis) p33
[102] LaMarr B, Bautz M, Kissel S, Prigozhin G, Hayashida K, Tsuru T and Matsumoto H 2004 *Ground calibration of X-ray CCD detectors with charge injection for the X-ray imaging spectrometer on Astro-E2 Proc. of SPIE* Vol15501 pp385-91
[103] CBCT electron density and image quality phantom (Computer Imaging Reference Systems, Inc) Website: www.imagingequipment.co.uk/downloadfile/742 Accessed on 3rd August 2011
[104] ISO 10360-1:2000 Geometrical product specifications (GPS) — Acceptance and reverification tests for coordinate measuring machines (CMM) —Part 1: Vocabulary, International Organization for Standardization
[105] ISO 10360-2:2009 Geometrical product specifications (GPS) — Acceptance and reverification tests for coordinate measuring machines (CMM) —Part 2: CMMs used for measuring linear dimensions, International Organization for Standardization
[106] ISO 10360-3:2000 Geometrical product specifications (GPS) — Acceptance and reverification tests for coordinate measuring machines (CMM) -- Part 3: CMMs with the axis of a rotary table as the fourth axis, International Organization for Standardization
[107] ISO 10360-4:2000 Geometrical product specifications (GPS) — Acceptance and reverification tests for coordinate measuring machines (CMM) —Part 4: CMMs used in scanning measuring mode, International Organization for Standardization
[108] ISO 10360-5:2010 Geometrical products specification (GPS) — Acceptance and reverification tests for coordinate measuring machines (CMM) — Part 5: CMMs

using single and multiple stylus probing systems, International Organization for Standardization
[109] ISO 10360-6:2001 Geometrical product specifications (GPS) — Acceptance and reverification tests for coordinate measuring machines (CMM) —Part 6: Estimation of errors in computing Gaussian associated features, International Organization for Standardization
[110] ISO 10360-7:2011 Geometrical product specifications (GPS) — Acceptance and reverification tests for coordinate measuring machines (CMM) -- Part 7: CMMs equipped with imaging probing systems, International Organization for Standardization
[111] Flack D 2011 *CMM verification* Measurement Good Practice Guide No. 42
[112] ISO 15708-2:2002(E) Non-destructive testing – Radiation methods – Computed tomography – Part 2: Examination practices, International Organization for Standardization
[113] ISO/TC 213 N 1346 Geometrical product specification (GPS) - Acceptance and and reverification tests for coordinate measuring machines (CMM) - Computed tomography, International Organization for Standardization
[114] ASTM E1695 - 95(2006)e1 Standard test method for measurement of computed tomography (CT) system performance, ASTM International
[115] ASTM E 1441 - 00 Standard guide for computed tomography (CT) imaging, ASTM International
[116] ASTM E 1570 - 11 Standard practice for computed tomography (CT) examination, ASTM International
[117] VDI/VDE 2630 Part 1.1:2009 Computed tomography in dimensional measurement - Basics and definitions, Institute for Innovation and Technology
[118] VDI/VDE 2630 Part 1.2:2010 Computed tomography in dimensional measurement - Influencing variables on measurement results and recommendations for computed tomography dimensional measurements, Institute for Innovation and Technology
[119] VDI/VDE 2630 Part 1.3:2011 Computed tomography in dimensional measurement - Guideline for the application of DIN EN ISO 10360 for coordinate measuring machines with CT-sensors, Institute for Innovation and Technology
[120] Ronchi V 1961 Resolving power of calculated and detected images *J. Opt. Soc. Am.* **51** 458-60
[121] den Dekker A J and van den Bos A 1997 Resolution: a survey *JOSA A: Optics, Image Science, and Vision* **14** 547-57
[122] Leach R K 2011 *Optical measurement of surface topography* (Springer) p323
[123] Yester M W and Barnes G T 1977 *Geometrical limitations of computed tomography (CT) scanner resolution Proc. of Applications of Optical instrumentation in medicine, SPIE* Vol127 pp296-303
[124] Sharma K S, Seshadri S, Feser M and Wang G 2010 *Accurate resolution measurement for X-ray micro-CT systems Proc. of X-Ray Microscopy* (Chicago)
[125] Grimmer R, Krause J, Karolczak M, Lapp R and Kachelrib M 2008 *Assessment of spatial resolution in CT Proc. of Nuclear Science Symposium and Medical Imaging Conference* (Dresden, Germany) pp5562 - 66
[126] Staude A and Goebbels J 2011 *Determining the spatial resolution in compute tomography – comparison of MTF and line-pair structures Proc. of International Symposium on Digital Industrial Radiology and Computed Tomography* (Berlin, Germany) pp9
[127] prEN 16016-3:2009: E Non destructive testing - Radiation methods - Computed tomography - Part 3: Operation and interpretation, Austrian Standards Institute
[128] Hanson K M 1981 Radiology of the skull and brain, Vol. 5: Technical aspects of computed tomography *113* Noise and contrast discrimination in computed tomography Newton T H and Potts D G
[129] Lida H, Sasaki H, Inoue H, Kanno I, Miura S, Okuyama D and Uemura K 1986 A simulation study to evaluate the statistical noise and spatial resolution in image

reconstruction of emission computed tomography--with respect to the optimization of the filter function in the convolution integral *Radioisotopes* **35** 589-94

[130] Bartscher M, Neukamm M, Hilpert U, Neuschaefer-Rube U, Härtig F, Kniel K, Ehrig K, Staude A and Goebbels J 2010 Achieving traceability of industrial computed tomography *Key. Eng. Mater.* **437** 79-83

[131] Neuschaefer-Rube U, Neugebauer M, Ehrig W, Bartscher M and Hilpert U 2008 Tactile and optical microsensors: test procedures and standards *Meas. Sci. Technol.* **19**

[132] Bartscher M, Hilpert U, Goebbels J and Weidemann G 2007 Enhancement and proof of accuracy of industrial computed tomography (CT) measurements *Ann. CIRP* **56** 495-98

[133] Bartscher M, Neukamm M, Koch M, Neuschaefer-Rube U, Staude A, Goebbels J, Ehrig K, Kuhn C and Deffner A 2010 *Performance assessment of geometry measurements with micro-CT using a dismountable work-piece-near reference standard Proc. of 10th European Conference on Non-Destructive Testing* (Moscow: NDT)

[134] Lettenbauer H, Weiss D and Georgi B 17th November 2009 Verification of the accuracy of computed tomography: systems for measuring 3-D technology Quality Digest Magazine www.qualitydigest.com/inside/metrology-article/verification-accuracy-computed-tomography.html#

[135] CT Audit:Interlaboratory comparison of computed tomography systems for dimensional metrology (Laboratory of Industrial and Geometrical Metrology, University of Padova) Website: static.gest.unipd.it/~carmignato/ct-audit/index.htm Accessed on 3rd August 2011

[136] Pierobon A and Carmignato S 2011 *Preliminary results of the 'CT Audit' project: First international intercomparison of computed tomography systems for dimensional metrology Proc. of International Symposium on Digital Industrial Radiology and Computed Tomography* (Berlin, Germany) pp8

[137] Carmignato S, Pierobon A and Savio E 2011 CT audit - interlaboratory comparison of computed tomography systems for dimensional metrology (University of Padova)

[138] Carmignato S, Dreossi D, Mancini L, Marinello F, Tromba G and Savio E 2009 Testing of X-ray microtomography systems using a traceable geometrical standard *Meas. Sci. Technol.* **20** 084021-28

[139] Kiekens K, Welkenhuyzen F, Tan Y, Bleys P, Voet A, Kruth J-P and Dewulf W 2011 A test object with parallel grooves for calibration and accuracy assessment of industrial computed tomography (CT) metrology *Meas. Sci. Technol.* **22** 115502-09

[140] Schmitt R and Niggemann C 2010 Uncertainty in measurement for x-ray-computed tomography using calibrated work pieces *Meas. Sci. Technol.* **21** 054008-17

[141] Schambach S J, Bag S, Schilling L, Groden C and Brockmann M A 2010 Application of micro-CT in small animal imaging *Methods* **50** 2-13